

TENSOR PRODUCTS OF A_∞ -ALGEBRAS WITH HOMOTOPY INNER PRODUCTS

THOMAS TRADLER¹ AND RONALD UMBLE²

ABSTRACT. We show that the tensor product of two cyclic A_∞ -algebras is, in general, not a cyclic A_∞ -algebra, but an A_∞ -algebra with homotopy inner product. More precisely, following Markl and Shnider in [MS], we construct an explicit combinatorial diagonal on the pairahedra, which are contractible polytopes controlling the combinatorial structure of an A_∞ -algebra with homotopy inner products, and use it to define a categorically closed tensor product. A cyclic A_∞ -algebra can be thought of as an A_∞ -algebra with homotopy inner products whose higher inner products are trivial. However, the higher inner products on the tensor product of cyclic A_∞ -algebras are not necessarily trivial.

1. INTRODUCTION

Let R be a commutative ring with unity and let $C_*(K)$ denote the cellular chains of associahedra $K = \sqcup_{n \geq 2} K_n$, see [S]. Identify $C_*(K)$ with the A_∞ -operad \mathcal{A}_∞ and consider the Sanedlidze-Umble (S-U) diagonal $\Delta_K : C_*(K) \rightarrow C_*(K) \otimes C_*(K)$ [SU]. Given A_∞ -algebras $(A, \mu_n)_{n \geq 1}$ and $(B, \nu_n)_{n \geq 1}$ over R , represent A and B as algebras over \mathcal{A}_∞ via operadic maps $\{\zeta_A : C_*(K_n) \rightarrow \text{Hom}(A^{\otimes n}, A)\}_{n \geq 1}$ and $\{\zeta_B : C_*(K_n) \rightarrow \text{Hom}(B^{\otimes n}, B)\}_{n \geq 1}$. Define $\varphi_1 = \mu_1 \otimes \mathbf{1} + \mathbf{1} \otimes \nu_1$ and

$$\varphi_n = [(\zeta_A \otimes \zeta_B) \Delta_K (e^{n-2})] \sigma_n,$$

where $\sigma_n : (A \otimes B)^{\otimes n} \rightarrow A^{\otimes n} \otimes B^{\otimes n}$ is the canonical permutation of tensor factors and e^{n-2} denotes the top dimensional cell of K_n . Then $(A \otimes B, \varphi_n)_{n \geq 1}$ is an A_∞ -algebra, and for example,

$$\varphi_2 = (\mu_2 \otimes \nu_2) \sigma_2 \quad \text{and} \quad \varphi_3 = [\mu_2(\mu_2 \otimes \mathbf{1}) \otimes \nu_3 + \mu_3 \otimes \nu_2(\mathbf{1} \otimes \nu_2)] \sigma_3.$$

An A_∞ -algebra (V, ρ_n) is *cyclic* if V is equipped with a cyclically invariant inner product $\langle -, - \rangle_V$, i.e., $\langle \rho_n(a_1, \dots, a_n), a_{n+1} \rangle_V = (-1)^\epsilon \langle \rho_n(a_2, \dots, a_{n+1}), a_1 \rangle_V$. Thus if (A, μ_n) and (B, ν_n) are cyclic, it is natural to ask whether $\langle -, - \rangle_A$ and $\langle -, - \rangle_B$ induce a cyclically invariant inner product on $(A \otimes B, \varphi_n)$. As a first approximation, consider the inner product

$$\langle a_1|b_1, a_2|b_2 \rangle_{A \otimes B} = (-1)^{|a_2||b_1|} \langle a_1, a_2 \rangle_A \langle b_1, b_2 \rangle_B,$$

which respects φ_1 and φ_2 but not φ_3 since

$$\langle \varphi_3(a_1|b_1, a_2|b_2, a_3|b_3), a_4|b_4 \rangle - (-1)^\epsilon \langle \varphi_3(a_2|b_2, a_3|b_3, a_4|b_4), a_1|b_1 \rangle \neq 0.$$

Date: August 25, 2011.

1991 Mathematics Subject Classification. 55S15, 52B05, 18D50, 55U99.

Key words and phrases. A_∞ -algebra with homotopy inner product, colored operad, cyclic A_∞ -algebra, diagonal, pairahedron, tensor product, W-construction.

¹ This research funded in part by the PSC-CUNY grant PSCREG-41-316.

² This research funded in part by a Millersville University faculty research grant.

However, there is a chain homotopy $\varrho_{2,0} : (A \otimes B)^{\otimes 4} \rightarrow R$ such that

$$\begin{aligned} (\varrho_{2,0} \circ d)(a_1|b_1, a_2|b_2, a_3|b_3, a_4|b_4) = \\ \langle \varphi_3(a_1|b_1, a_2|b_2, a_3|b_3), a_4|b_4 \rangle - (-1)^\epsilon \langle \varphi_3(a_2|b_2, a_3|b_3, a_4|b_4), a_1|b_1 \rangle, \end{aligned}$$

where d is the linear extension of φ_1 and

$$\varrho_{2,0}(x_1|y_1, x_2|y_2, x_3|y_3, x_4|y_4) = \pm \langle \mu_3(x_1, x_2, x_3), x_4 \rangle_A \langle y_1, \nu_3(y_2, y_3, y_4) \rangle_B.$$

Thus $\langle -, - \rangle_{A \otimes B}$ respects φ_3 up to a homotopy, and there is hope.

In [T1], the first author defined the notion of an A_∞ -algebra with homotopy inner product, which is an A_∞ -algebra (A, μ_n) together with “compatible” families of module maps

$$\{\lambda_{j,k} : A^{\otimes j} \otimes A \otimes A^{\otimes k} \rightarrow A\}_{j,k \geq 0}$$

and higher inner products

$$\{\varrho_{j,k} : A \otimes A^{\otimes j} \otimes A \otimes A^{\otimes k} \rightarrow R\}_{j,k \geq 0}.$$

Homotopy inner products appear in actions on moduli spaces (*e.g.* [T2, TZ]), in the deformation theory of inner products [TT], and in symplectic structures on formal non-commutative supermanifolds [C].

Following the construction of Markl and Shnider in [MS], we extend the inner product $\langle -, - \rangle_{A \otimes B}$ defined above to a homotopy inner product on $(A \otimes B, \varphi_n)$ as follows:

- (1) We identify the cellular chains of the associahedra and pairahedra with a three-colored operad $C_*\hat{\mathcal{A}}$ (the pairahedra, constructed by the first author in [T1], encode the relations among A_∞ -operations, module maps, and homotopy inner products).
- (2) We adapt Boardman and Vogt’s W -construction [BV] to obtain the three-colored operad $Q_*\hat{\mathcal{A}}$, which is a cubical decomposition of $C_*\hat{\mathcal{A}}$.
- (3) We define a quasi-invertible subdivision map $q : C_*\hat{\mathcal{A}} \rightarrow Q_*\hat{\mathcal{A}}$ whose quasi-inverse $p : Q_*\hat{\mathcal{A}} \rightarrow C_*\hat{\mathcal{A}}$ is defined in terms of an appropriate partial ordering on binary planar diagrams.
- (4) The Serre diagonal on cellular chains of the n -cube induces a coassociative diagonal $\Delta_Q : Q_*\hat{\mathcal{A}} \rightarrow Q_*\hat{\mathcal{A}} \otimes Q_*\hat{\mathcal{A}}$, which in turn induces a non-coassociative diagonal

$$\Delta_C : C_*\hat{\mathcal{A}} \xrightarrow{q} Q_*\hat{\mathcal{A}} \xrightarrow{\Delta_Q} Q_*\hat{\mathcal{A}} \otimes Q_*\hat{\mathcal{A}} \xrightarrow{p \otimes p} C_*\hat{\mathcal{A}} \otimes C_*\hat{\mathcal{A}}.$$

- (5) We represent the homotopy inner products on A and B as operadic maps $\psi_A : C_*\hat{\mathcal{A}} \rightarrow \mathcal{E}nd_A$ and $\psi_B : C_*\hat{\mathcal{A}} \rightarrow \mathcal{E}nd_B$, and define

$$\psi_{A \otimes B} : C_*\hat{\mathcal{A}} \xrightarrow{\Delta_C} C_*\hat{\mathcal{A}} \otimes C_*\hat{\mathcal{A}} \xrightarrow{\psi_A \otimes \psi_B} \mathcal{E}nd_A \otimes \mathcal{E}nd_B \xrightarrow{\cong} \mathcal{E}nd_{A \otimes B}.$$

The paper is organized as follows. Section 2 defines the three-colored operads $C_*\hat{\mathcal{A}}$ and $Q_*\hat{\mathcal{A}}$. The map $q : C_*\hat{\mathcal{A}} \rightarrow Q_*\hat{\mathcal{A}}$ is defined in Section 3 and a quasi-inverse p is defined in Section 4. Section 5 introduces the diagonal Δ_C , and we conclude the paper with some computations in Section 6. To maximize accessibility, longer proofs and other technical considerations are collected in the appendices. Signs are discussed in Appendix A; the contractibility of pairahedra is proved in Appendix B; the fact that relation “ \leq ” in the definition of the morphism p is a partial ordering is

established in Appendix C; and the fact that p is a chain map is proved in Appendix D.

2. THE THREE-COLORED OPERADS $C_*\hat{\mathcal{A}}$ AND $Q_*\hat{\mathcal{A}}$

In this section we construct the three-colored operads $C_*\hat{\mathcal{A}}$ and $Q_*\hat{\mathcal{A}}$. Algebras over $C_*\hat{\mathcal{A}}$ are A_∞ -algebras with homotopy inner products and $Q_*\hat{\mathcal{A}}$ is a cubical subdivision of $C_*\hat{\mathcal{A}}$. Both operads are defined in terms of three types of planar diagrams: (1) *planar trees*, which encode the homotopy associativity structure, (2) *module trees*, which encode the homotopy bimodule structure, and (3) *inner product diagrams*, which encode the homotopy inner product structure. We shall refer to a diagram in any of these categories as a *planar diagram*. The term *leaf* of a planar diagram will always refer to an external inward directed edge; the term *root* will always refer to the single external outward directed edge of a tree; and the term *edge* will always refer to an internal edge, which is neither a root nor a leaf.

Planar diagrams are generated by three families of corollas: $\{T_n\}_{n \geq 2}$, $\{M_{j,k}\}_{j+k \geq 0}$, and $\{I_{j,k}\}_{j+k \geq 0}$. The root and leaves of a corolla have one of three colors: *thick*, *thin*, or *empty*. The corolla T_n has n thin leaves and a thin root; $M_{j,k}$ has a thick vertical root, a thick vertical leaf, j thin leaves in the left half-plane, and k thin leaves in the right half-plane; and $I_{j,k}$ has an empty root, which is graphically represented by a thick vertex, two thick horizontal leaves, j thin leaves in the upper half-plane, and k thin leaves in the lower half-plane, all meeting at the thick vertex. An example of each type appears in Figure 1.

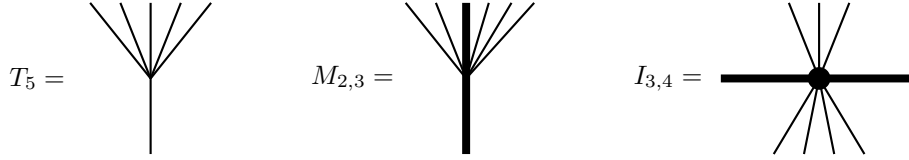


FIGURE 1. Three types of corollas

A planar tree T is composed with a diagram D by attaching the root of T to a thin leaf of D . Two module trees are composed by attaching the thick root of one to the thick leaf of the other. A module tree M is composed with an inner product diagram I by attaching the thick root of M to a thick leaf of I . Two inner product diagrams cannot be composed. A planar diagram resulting from each of the various compositions appears in Figure 2.

Given a planar diagram D , let $\mathcal{L}(D)$ denote the set of leaves of D . If $k = \#\mathcal{L}(D)$, we use a bijection $f : \{1, \dots, k\} \rightarrow \mathcal{L}(D)$ to index the elements of $\mathcal{L}(D)$. In particular, the symbol f_\circlearrowleft denotes the “canonical” indexing, which numbers the leaves of a (planar or module) tree from left to right and the leaves of an inner product diagram clockwise starting from the left thick leaf (see Figure 3).

Let $\mathcal{E}(D)$ denote the set of (internal) edges of a planar diagram D .

Definition 2.1. Define the **orientation** of a corolla to be $+1$ or -1 ; an **orientation** of a planar diagram D with $\mathcal{E}(D) = \{e_1, \dots, e_k\}$ is a formal skew-commutative product $\omega = e_{i_1} \wedge \dots \wedge e_{i_k}$. Thus D admits exactly two orientations: ω and $-\omega$.

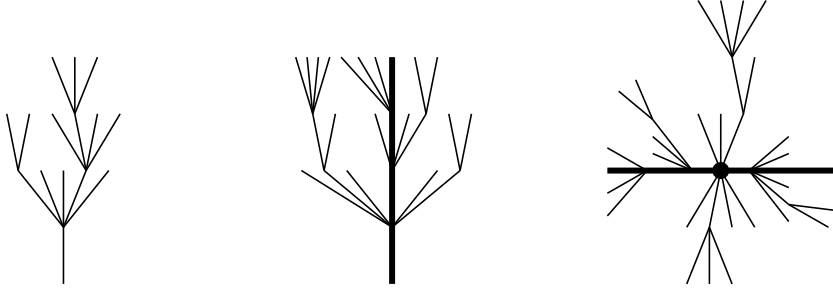


FIGURE 2. Three types of planar diagrams (a tree diagram T , a module diagram M , an inner product diagram I)

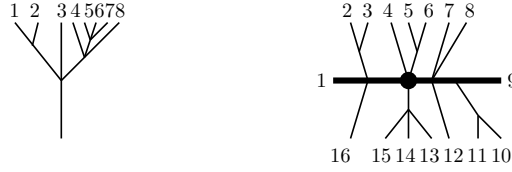


FIGURE 3. Canonical numbering f_{\circ} of the leaves of a diagram

Following the construction of the colored operad governing homotopy inner products in [LT], we define the three-colored operad $C_*\hat{\mathcal{A}}$. Let $\mathbb{Z}_3 = \{0, 1, 2\}$, and denote the empty color by 0, the thin color by 1, and the thick color by 2.

Definition 2.2. The three-colored operad

$$C_*\hat{\mathcal{A}} = \bigoplus_{\substack{\mathbf{x} \times \mathbf{y} \in \mathbb{Z}_3^{n+1} \\ n \geq 1}} C_*\hat{\mathcal{A}}_{\mathbf{y}}^{\mathbf{x}},$$

is the graded R -module in which $C_*\hat{\mathcal{A}}_{\mathbf{y}}^{\mathbf{x}} = 0$ unless

(i) $\mathbf{x} \times \mathbf{y} = 1 \cdots 1 \times 1 \in \mathbb{Z}_3^{n+1}$:

$C_*\hat{\mathcal{A}}_{\mathbf{y}}^{\mathbf{x}}$ is generated by triples (T, f, ω) modulo $(T, f, -\omega) = -(T, f, \omega)$, where T is a planar tree with n leaves and ω is an orientation on T .

(ii) $\mathbf{x} \times \mathbf{y} = 1 \cdots 121 \cdots 1 \times 2 \in \mathbb{Z}_3^{n+1}$ with 2 in the i^{th} position of \mathbf{x} :

$C_*\hat{\mathcal{A}}_{\mathbf{y}}^{\mathbf{x}}$ is generated by triples (M, f, ω) modulo $(M, f, -\omega) = -(M, f, \omega)$, where M is a module tree with n leaves of which $f(i)$ is thick, and ω is an orientation on M .

(iii) $\mathbf{x} \times \mathbf{y} = 1 \cdots 121 \cdots 121 \cdots 1 \times 0 \in \mathbb{Z}_3^{n+1}$ with 2 in the i^{th} and j^{th} positions:

$C_*\hat{\mathcal{A}}_{\mathbf{y}}^{\mathbf{x}}$ is generated by triples (I, f, ω) modulo $(I, f, -\omega) = -(I, f, \omega)$, where I is an inner product diagram with n leaves of which $f(i)$ and $f(j)$ are thick, and ω is an orientation on I .

The **coloring** of a generator $(D, f, \omega) \in C_*\hat{\mathcal{A}}_{\mathbf{y}}^{\mathbf{x}}$ is the pair $\mathbf{x} \times \mathbf{y}$, and its **degree**

$$|(D, f, \omega)| := \#\mathcal{L}(D) - \#\mathcal{E}(D) - 2.$$

When $|(D, f, \omega)| = n$, we write $(D, f, \omega) \in C_n \hat{\mathcal{A}}$. Formally adjoin **units** to $C_* \hat{\mathcal{A}}$ and define their degrees to be 0. Given an edge $e \in \mathcal{E}(D)$, let D/e denote the planar diagram obtained from D by contracting e to a point. Define the **boundary** of (D, f, ω) by

$$\partial_C(D, f, \omega) := \sum_{\substack{D'/e'=D \\ e' \in \mathcal{E}(D')}} (D', f, e' \wedge \omega),$$

summed over all diagrams D' and all edges $e' \in \mathcal{E}(D')$ such that $D'/e' = D$. The relation $\partial_C^2 = 0$ follows from the fact that $e' \wedge e'' \wedge \omega = -e'' \wedge e' \wedge \omega$. If $n = \#\mathcal{L}(D)$ and $\sigma \in S_n$, define the S_n -**action** by

$$\sigma \cdot (D, f, \omega) := \text{sgn}(\sigma) \cdot (D, f \circ \sigma, \omega).$$

Given generators $(D, f_D, \omega_D) \in C_m \hat{\mathcal{A}}$ and $(E, f_E, \omega_E) \in C_n \hat{\mathcal{A}}$, let $k = \#\mathcal{L}(D)$ and $l = \#\mathcal{L}(E)$. For $1 \leq i \leq k$, define the i^{th} **operadic composition** $(D, f_D, \omega_D) \circ_i (E, f_E, \omega_E)$ to be zero unless the root of E and the i^{th} input of D have the same color, in which case,

$$(2.1) \quad (D, f_D, \omega_D) \circ_i (E, f_E, \omega_E) := (-1)^\epsilon (D \circ_{f_D(i)} E, f_{D \circ E}, \omega_D \wedge \omega_E \wedge e),$$

where $\epsilon = i(l+1) + kn$, $D \circ_{f_D(i)} E$ is obtained by attaching the root of E to leaf $f_D(i)$ of D , “ e ” denotes the new edge, and

$$f_{D \circ E}(j) = \begin{cases} f_D(j), & 1 \leq j < i, \\ f_E(j-i+1), & i \leq j < i+l, \\ f_D(j-l+1), & i+l \leq j \leq k+l-1. \end{cases}$$

For a justification of the sign $(-1)^\epsilon$, refer to Equations (A.1), (A.2), (A.3), and Definition A.2 in Appendix A.1.

We need the following “metric refinement” of $C_* \hat{\mathcal{A}}$ generated by diagrams whose edges are labeled either m (metric) or n (non-metric):

Definition 2.3. The **three-colored operad**

$$Q_* \hat{\mathcal{A}} = \bigoplus_{\substack{\mathbf{x} \times \mathbf{y} \in \mathbb{Z}_3^{n+1} \\ n \geq 1}} Q_* \hat{\mathcal{A}}_{\mathbf{y}}^{\mathbf{x}},$$

is the graded R -module generated by tuples (D, f, g, ω) modulo $(D, f, g, -\omega) = -(D, f, g, \omega)$, where D and f are as in Definition 2.2 and $g : \mathcal{E}(D) \rightarrow \{m, n\}$ labels the edges in D (if D is a corolla, g is the empty map). The **metric edges** of D form the set $\mathcal{M}(D) = g^{-1}(m)$; all other edges are **non-metric**. If $\mathcal{M}(D) = \{e_1, \dots, e_l\}$, an **orientation** of D is a formal skew-commutative product $\omega = e_{i_1} \wedge \dots \wedge e_{i_l}$, and the **degree** $|(D, f, g, \omega)| := \#\mathcal{M}(D)$. **Units** are inherited from $C_* \hat{\mathcal{A}}$ and the **boundary** is given by

$$\begin{aligned} \partial_Q(D, f, g, e_{i_1} \wedge \dots \wedge e_{i_l}) := \\ \sum_{j=1}^l (-1)^j \left[(D/e_{i_j}, f, g/e_{i_j}, e_{i_1} \wedge \dots \wedge \hat{e}_{i_j} \wedge \dots \wedge e_{i_l}) - (D_{e_{i_j}}, f, g_{e_{i_j}}, e_{i_1} \wedge \dots \wedge \hat{e}_{i_j} \wedge \dots \wedge e_{i_l}) \right], \end{aligned}$$

where $g/e_{i_j}(e) = g(e)$ if $e \neq e_{i_j}$, $D_{e_{i_j}}$ is obtained from D by relabeling e_{i_j} non-metric (n), and $g_{e_{i_j}}$ is the corresponding relabeling. It is straightforward to check that $\partial_Q^2 = 0$. This time the S_k -**action** is given by $\sigma \cdot (D, f, g, \omega) = (D, f \circ \sigma, g, \omega)$,

and the **coloring** of $(D, f, g, \omega) \in Q_*\hat{\mathcal{A}}_y^{\mathbf{x}}$ is the pair $\mathbf{x} \times y$. Given generators (D, f_D, g_D, ω_D) and (E, f_E, g_E, ω_E) , define the i^{th} **operadic composition** $(D, f_D, g_D, \omega_D) \circ_i (E, f_E, g_E, \omega_E)$ to be zero unless the root of E and the i^{th} leaf of D have the same color, in which case

$$(D, f_D, g_D, \omega_D) \circ_i (E, f_E, g_E, \omega_E) := (D \circ_{f_D(i)} E, f_{D \circ E}, g_{D \circ E}, \omega_D \wedge \omega_E),$$

where $D \circ_{f_D(i)} E$ is defined as in Definition 2.2 and

$$g_{D \circ E}(e) = \begin{cases} n, & e \text{ is the new edge} \\ g_D(e), & e \in \mathcal{E}(D) \\ g_E(e), & e \in \mathcal{E}(E). \end{cases}$$

For comparison, note that the sign prefixes that appear in the formulas defining the S_k -action and \circ_i -composition in $C_*\hat{\mathcal{A}}$, do not appear correspondingly in $Q_*\hat{\mathcal{A}}$. Figure 4 on page 13 displays a graphical representation of the combinatorial relationships among the generators in $Q_*\hat{\mathcal{A}}_0^{2112}$; this clearly illustrates the boundary ∂_Q . As we shall see in the next section, $C_*\hat{\mathcal{A}}$ and $Q_*\hat{\mathcal{A}}$ are operadically quasi-isomorphic.

3. THE MAP $q : C_*\hat{\mathcal{A}} \rightarrow Q_*\hat{\mathcal{A}}$

In this section, we define an operadic map $q : C_*\hat{\mathcal{A}} \rightarrow Q_*\hat{\mathcal{A}}$ and show that it is a quasi-isomorphism. Our proof depends on the fact that pairahedra are contractible. Let ω_B^{std} denote the standard orientation on a binary diagram $B \in C_0\hat{\mathcal{A}}$ defined in Appendix A.2, and let m denote the constant map $g(e) = m$.

Definition 3.1. Define $q : C_*\hat{\mathcal{A}} \rightarrow Q_*\hat{\mathcal{A}}$ as follows:

- (i) On units, define q to be the identity.
- (ii) On a corolla $(c, f_{\circlearrowleft}, +1) \in C_*\hat{\mathcal{A}}_y^{\mathbf{x}}$, define

$$q(c, f_{\circlearrowleft}, +1) = \sum_{B \in C_0\hat{\mathcal{A}}_y^{\mathbf{x}}} (B, f_{\circlearrowleft}, m, \omega_B^{\text{std}}).$$

- (iii) Decompose a generator $(D, f, \omega) \in C_*\hat{\mathcal{A}}$ as a \circ_i -composition of corollas, and define $q(D, f, \omega)$ by extending S_k -equivariantly and \circ_i -multiplicatively, *i.e.*,

$$\begin{aligned} q(\sigma \cdot (D, f, \omega)) &= \sigma \cdot q(D, f, \omega); \\ q((E, f, \omega) \circ_i (E', f', \omega')) &= q(E, f, \omega) \circ_i q(E', f', \omega'). \end{aligned}$$

This extension is well-defined since $C_*\hat{\mathcal{A}}$ is freely generated by corollas $(c, f_{\circlearrowleft}, +1)$ (modulo the relation $(\dots, -\omega) = -(\dots, \omega)$).

By definition, q respects units, the S_k -action, and \circ_i -composition. And furthermore:

Proposition 3.2. *The map $q : C_*\hat{\mathcal{A}} \rightarrow Q_*\hat{\mathcal{A}}$ is a chain map.*

Proof. Since ∂_C and ∂_Q respect S_k -actions and act as derivations of \circ_i , it is sufficient to check the result on a corolla $(c, f_{\circlearrowleft}, +1) \in C_*\hat{\mathcal{A}}_y^{\mathbf{x}}$:

$$q(\partial_C(c, f_{\circlearrowleft}, +1)) = \sum_{D/e=c} q(D, f_{\circlearrowleft}, e)$$

$$\begin{aligned}
 &= \sum_{\substack{D/e=c, \\ (D, f_\circ, e) = (-1)^{\epsilon_1} \sigma \cdot [(c', f'_\circ, 1) \circ_j (c'', f''_\circ, 1)] \\ (c', f'_\circ, 1) \in C_* \hat{\mathcal{A}}_{y'}^{\mathbf{x}'}; (c'', f''_\circ, 1) \in C_* \hat{\mathcal{A}}_{y''}^{\mathbf{x}''}}} (-1)^{\epsilon_1} \sigma \cdot [q(c', f'_\circ, 1) \circ_j q(c'', f''_\circ, 1)] \\
 &= \sum_{\substack{B' \in C_0 \hat{\mathcal{A}}_{y'}^{\mathbf{x}'}, \\ B'' \in C_0 \hat{\mathcal{A}}_{y''}^{\mathbf{x}''}}} (-1)^{\epsilon_1} \sigma \cdot [(B', f'_\circ, m, \omega_{B'}^{\text{std}}) \circ_j (B'', f''_\circ, m, \omega_{B''}^{\text{std}})] \\
 &= \sum_{\substack{(B, f_\circ, g, \omega_j) \in Q_* \hat{\mathcal{A}}_y^{\mathbf{x}} \\ \#g^{-1}(n)=1}} (-1)^{\epsilon_2} (B, f_\circ, g, \omega_j),
 \end{aligned}$$

where ϵ_2 is a function of ϵ_1 , and both signs are computed in Appendix A.3. The last expression is summed over all binary diagrams B with exactly one non-metric edge (the one coming from the composition \circ_j) and ω_j is the induced orientation. On the other hand,

$$\begin{aligned}
 (3.1) \quad \partial_Q(q(c, f_\circ, +1)) &= \sum_{B \in C_0 \hat{\mathcal{A}}_y^{\mathbf{x}}} \partial_Q(B, f_\circ, m, \omega_B^{\text{std}} = e_1 \wedge \cdots \wedge e_k) \\
 &= \sum_B \sum_{e_i} (-1)^i \left[(B/e_i, f_\circ, m/e_i, \omega_B^{\hat{e}_i}) - (B_{e_i}, f_\circ, g_{e_i}, \omega_B^{\hat{e}_i}) \right],
 \end{aligned}$$

where $\omega_B^{\hat{e}_i} = e_1 \wedge \cdots \wedge \hat{e}_i \wedge \cdots \wedge e_k$. First, we claim that the “ B/e_i ” terms cancel. To see this, note that if e_i is an edge of a binary diagram B , there is second binary diagram B' and an edge e' in B' such that $B'/e' = B/e_i$. In fact, B and B' are related by one of the 6 local moves depicted in Definition 4.1 (if $B < B'$, obtain B/e_i by collapsing the edges within the two circles). Thus for purposes of orientation, we may symbolically identify e' with e_i and express their standard orientations as $\omega_B^{\text{std}} = e_1 \wedge \cdots \wedge e_i \wedge \cdots \wedge e_k$ and $\omega_{B'}^{\text{std}} = -e_1 \wedge \cdots \wedge e_i \wedge \cdots \wedge e_k$. Consequently, each “ B/e_i ” term appears twice with opposite signs. Formula (3.1) now simplifies to

$$\partial_Q(q(c, f_\circ, 1)) = \sum_B \sum_{e_i} (-1)^{i+1} (B_{e_i}, f_\circ, g_{e_i}, \omega_B^{\hat{e}_i}) = q(\partial_C(c, f_\circ, 1)),$$

summed over all binary diagrams B with exactly one non-metric edge e_i ; the fact that $(-1)^{i+1} \omega_B^{\hat{e}_i} = (-1)^{\epsilon_2} \omega_j$ is verified in Appendix A.3. \square

The fact that q is a quasi-isomorphism follows from the next proposition.

Proposition 3.3. *The polytopes associated with T_n , $M_{k,l}$, and $I_{k,l}$ are contractible.*

The proof of Proposition 3.3 is technical and appears in Appendix B.

Corollary 3.4. *The map $q : C_* \hat{\mathcal{A}} \rightarrow Q_* \hat{\mathcal{A}}$ is a quasi-isomorphism of operads.*

Proof. Since q is a chain map respecting the S_k -action, \circ_i -composition, and units, it is operadic. Furthermore, $q_y^{\mathbf{x}} : C_* \hat{\mathcal{A}}_y^{\mathbf{x}} \rightarrow Q_* \hat{\mathcal{A}}_y^{\mathbf{x}}$ is a quasi-isomorphism for each pair $\mathbf{x} \times y$ by Proposition 3.3 (c.f. [BV]). \square

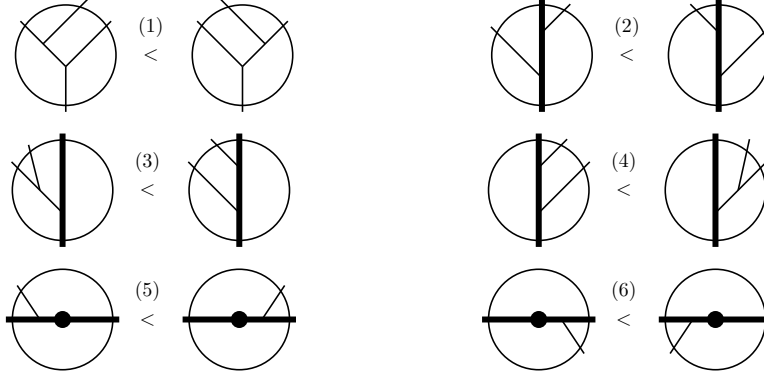
Geometrically, $C_* \hat{\mathcal{A}}$ is represented by the cellular chains of the various polytopes mentioned above, $Q_* \hat{\mathcal{A}}$ is represented by the cellular chains of an appropriate subdivision, and the morphism q associates each cell of $C_* \hat{\mathcal{A}}$ with the sum of cells in

its subdivision (*c.f.* Figure 4). However, constructing a quasi-inverse of q requires us to make a choice, which we shall do in the next section.

4. THE MAP $p : Q_*\hat{\mathcal{A}} \rightarrow C_*\hat{\mathcal{A}}$

In this section, we define a quasi-inverse p of the morphism q defined in the previous section. Our strategy is to extend the usual Tamari partial ordering on planar binary trees to the set \mathcal{B} of all planar binary diagrams. Given a planar diagram D , let \mathcal{B}_D denote the subposet of \mathcal{B} given by applying all possible sequences of edge insertions to D . Then \mathcal{B}_D has a unique minimal element D_{\min} and maximal element D_{\max} (Lemma 4.2), and p applied to a diagram D is the sum of all diagrams S such that $S_{\max} \leq D_{\min}$ (Definition 4.4).

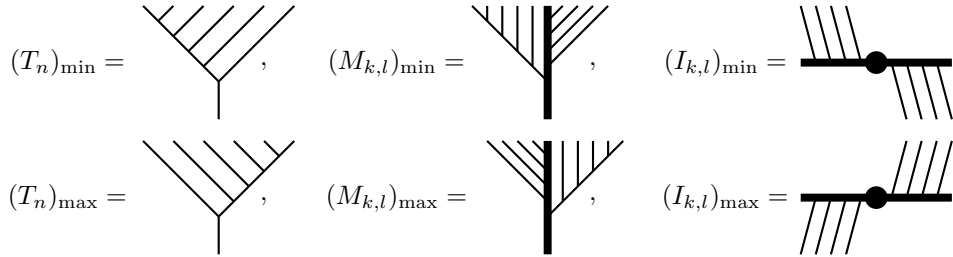
Definition 4.1. A pair of binary diagrams $(B_1, B_2) \in \mathcal{B} \times \mathcal{B}$ is an **edge-pair** if B_1 and B_2 differ only within a single neighborhood in one of the following six possible ways:



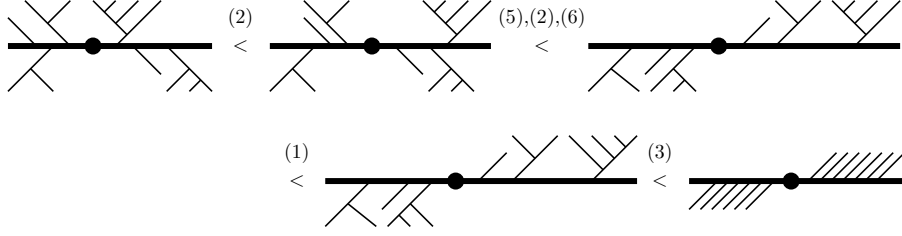
The set of all edge-pairs (B_1, B_2) generate a partial order “ \leq ” on \mathcal{B} ; for a proof see Appendix C.

Lemma 4.2. *The subposet \mathcal{B}_D has a unique minimal element D_{\min} and maximal element D_{\max} .*

Proof. Applying all possible sequences of edge insertions to a corolla c generates the subposet \mathcal{B}_c of binary diagrams with unique minimal and maximal elements of the following types:



Given a diagram $D \in \mathcal{B}$, there is always a sequence of inequalities in \mathcal{B}_D from D_{\min} to D_{\max} . For example,



Since every diagram D decomposes as a \circ_i -composition of corollas, the conclusion follows. \square

Remark 4.3. The six local inequalities in Definition 4.1 define one of 2^6 such local systems, some of which fail to generate a partial order on \mathcal{B} . Of those that do, some fail to satisfy the conclusion of Lemma 4.2. However, any partial order generated by one of these local systems can be used to construct the desired quasi-inverse p provided it satisfies the conclusion of Lemma 4.2.

We are ready to define the operadic quasi-inverse $p : Q_*\hat{\mathcal{A}} \rightarrow C_*\hat{\mathcal{A}}$. We shall refer to a diagram with strictly metric edges as a *fully metric* diagram.

Definition 4.4. Define $p : Q_*\hat{\mathcal{A}} \rightarrow C_*\hat{\mathcal{A}}$ on generators as follows:

- (i) On units, define p to be the identity.
- (ii) On a fully metric diagram $(D, f_\circ, m, \omega_D) \in Q_k\hat{\mathcal{A}}_y^x$, define

$$p(D, f_\circ, m, \omega_D) = \sum_{\substack{(S, f_\circ, \omega(S, D)) \in C_k\hat{\mathcal{A}}_y^x \\ S_{\max} \leq D_{\min}}} (S, f_\circ, \omega(S, D)),$$

where $\omega(S, D)$ is the induced orientation defined in A.2.

- (iii) Decompose a generator $(D, f, g, \omega) \in Q_*\hat{\mathcal{A}}$ with non-metric edges as a \circ_i -composition of fully metric diagrams, and define $p(D, f, g, \omega)$ by extending S_k -equivariantly and \circ_i -multiplicatively, *i.e.*,

$$\begin{aligned} p(\sigma \cdot (D, f, g, \omega)) &= \sigma \cdot (D, f, g, \omega), \\ p((E, f, g, \omega) \circ_i (E', f', g', \omega')) &= p(E, f, g, \omega) \circ_i p(E', f', g', \omega'). \end{aligned}$$

Lemma 4.5. Let $(c, f, g, 1) \in Q_*\hat{\mathcal{A}}$ be a corolla, let $(B, f, m, \omega_B^{\text{std}}) \in Q_*\hat{\mathcal{A}}$ be a fully metric binary diagram, and let $\omega(c_{\min}, c)$ be the orientation of c_{\min} given by Equation (A.4) in A.2. Then

- (i) $p(c, f, g, 1) = (c_{\min}, f, \omega(c_{\min}, c))$.
- (ii) $p(B, f, m, \omega_B^{\text{std}}) = \begin{cases} (c, f, 1), & \text{if } B = c_{\max} \\ 0, & \text{otherwise.} \end{cases}$

Proof. (i) Let $(S, f, \omega) \in C_*\hat{\mathcal{A}}$ be a summand of $p(c, f, g, 1)$. Then $|(S, f, \omega)| = |(c, f, g, 1)| = 0$, which implies $\#\mathcal{L}(S) = \#\mathcal{E}(S) + 2$. Thus S is a binary diagram and $S = S_{\max}$. Since c is a corolla, $S = S_{\max} \leq c_{\min}$ implies $S = c_{\min}$; hence $p(c, f, g, 1) = (c_{\min}, f, \omega(c_{\min}, c))$.

(ii) Let $(B, f, m, \omega_B^{\text{std}}) \in Q_k\hat{\mathcal{A}}$ be a fully metric binary diagram and let $(S, f, \omega) \in C_k\hat{\mathcal{A}}$ be a summand of $p(B, f, m, \omega_B^{\text{std}})$. Then $B = B_{\min}$ has $k + 2$ leaves and k strictly metric edges so that $k = |(B, f, m, \omega_B^{\text{std}})| = |(S, f, \omega)| = (k + 2) - \#\mathcal{E}(S) - 2$.

But $\#\mathcal{E}(S) = 0$ implies $S = c$ is a corolla. The condition $c_{\max} \leq B_{\min} = B$ shows that when B is not a maximum, $p(B, f, m, \omega_B^{\text{std}}) = 0$; otherwise $p(B, f, m, \omega_B^{\text{std}}) = (c, f, +1)$ (the fact that $\omega(c, c_{\max}) = +1$ is verified in Equation (A.5) in A.2. \square

Proposition 4.6. *The map $p : Q_*\hat{\mathcal{A}} \rightarrow C_*\hat{\mathcal{A}}$ is a chain map.*

A rather lengthy proof of Proposition 4.6 appears in Appendix D.

Proposition 4.7. *The composition $pq = \text{Id}_{C_*\hat{\mathcal{A}}}$, and there is a chain homotopy from the identity $\text{Id}_{Q_*\hat{\mathcal{A}}}$ to the composition qp . Thus, p and q are operadic chain homotopy equivalences.*

Proof. Since p and q respect \circ_i -compositions and $C_*\hat{\mathcal{A}}$ is generated by \circ_i -compositions of corollas, it is sufficient to check pq on a corolla $(c, f, 1) \in C_*\hat{\mathcal{A}}_y^x$. With Lemma 4.5 (ii), we calculate

$$p(q(c, f, 1)) = \sum_{B \in C_0\hat{\mathcal{A}}_y^x} p(B, f, m, \omega_B^{\text{std}}) = p(c_{\max}, f, m, \omega_{c_{\max}}^{\text{std}}) = (c, f, 1).$$

On the other hand, we construct a chain homotopy $S : Q_*\hat{\mathcal{A}} \rightarrow Q_*\hat{\mathcal{A}}$, such that $\partial_Q S + S\partial_Q = qp - \text{Id}_{Q_*\hat{\mathcal{A}}}$. The chain homotopy $S : Q_n\hat{\mathcal{A}} \rightarrow Q_{n+1}\hat{\mathcal{A}}$ is defined by induction on the degree n . For $n = 0$, and the corolla $(c, f, g, 1) \in Q_0\hat{\mathcal{A}}$, Lemma 4.5(i) shows that

$$q(p(c, f, g, 1)) = q(c_{\min}, f, \omega(c_{\min}, c)) = (c_{\min}, f, n, 1),$$

where n is the constant non-metric assignment. The last sign follows from Equation (A.4), $\omega(c_{\min}, c) = \xi_{c_{\min}}$, and the description of $\xi_{c_{\min}}$ given in Remark A.7. Since, by Proposition 3.3, all pairahedra are contractible, we can find a path $S(c, f, g, 1) \in Q_1\hat{\mathcal{A}}$ with boundary endpoints $(qp)(c, f, g, 1) = (c_{\min}, f, n, 1)$ and $(c, f, g, 1)$, so that with $\partial_Q(c, f, g, 1) = 0$, we have:

$$(\partial_Q S + S\partial_Q)(c, f, g, 1) = (qp - \text{Id}_{Q_*\hat{\mathcal{A}}})(c, f, g, 1).$$

Note that qp is \circ_i -multiplicative and we extend S to all of $Q_0\hat{\mathcal{A}}$ as an (Id, qp) -derivation. With this, $\partial_Q S + S\partial_Q = qp - \text{Id}_{Q_*\hat{\mathcal{A}}}$ holds on all of $Q_0\hat{\mathcal{A}}$.

Inductively, assume that for all $k < n$, the map S has been extended as a chain homotopy from $\text{Id}_{Q_*\hat{\mathcal{A}}}$ to qp on $Q_k\hat{\mathcal{A}}$. Then, on $Q_n\hat{\mathcal{A}}$,

$$\begin{aligned} \partial_Q (qp - \text{Id}_{Q_*\hat{\mathcal{A}}} - S\partial_Q) &= (qp - \text{Id}_{Q_*\hat{\mathcal{A}}}) \partial_Q - \partial_Q S \partial_Q \\ &= (qp - \text{Id}_{Q_*\hat{\mathcal{A}}} - \partial_Q S) \partial_Q = S \partial_Q^2 = 0. \end{aligned}$$

Thus, since the pairahedra are contractible, for every fully metric diagram $(D, f, m, \omega) \in Q_n\hat{\mathcal{A}}$ the expression $(qp - \text{Id}_{Q_*\hat{\mathcal{A}}} - S\partial_Q)(D, f, m, \omega) \in Q_n\hat{\mathcal{A}}$ is a boundary. Choose $(D', f', g', \omega') \in Q_{n+1}\hat{\mathcal{A}}$ such that $\partial_Q(D', f', g', \omega') = (qp - \text{Id}_{Q_*\hat{\mathcal{A}}} - S\partial_Q)(D, f, m, \omega)$ and define $S(D, f, m, \omega) = (D', f', g', \omega')$. Then $(qp - \text{Id}_{Q_*\hat{\mathcal{A}}} - S\partial_Q - \partial_Q S)(D, f, m, \omega) = 0$. Finally, extend S to all of $Q_n\hat{\mathcal{A}}$ as a $(\text{Id}_{Q_*\hat{\mathcal{A}}}, qp)$ -derivation; then $S\partial_Q + \partial_Q S = qp - \text{Id}_{Q_*\hat{\mathcal{A}}}$ holds on $Q_n\hat{\mathcal{A}}$ by a straightforward calculation. Hence $S : qp \simeq \text{Id}_{Q_*\hat{\mathcal{A}}}$. \square

5. THE DIAGONAL $\Delta_C : C_*\hat{\mathcal{A}} \rightarrow C_*\hat{\mathcal{A}} \otimes C_*\hat{\mathcal{A}}$

Let I^n denote the standard n -cube, let $I = \sqcup_n I^n$ and let $C_*(I)$ denote cellular chains. The Serre diagonal $\Delta_I : C_*(I) \rightarrow C_*(I) \otimes C_*(I)$ acts on each cube I^n of the cubical complex $Q_*\hat{\mathcal{A}}$ and induces a coassociative diagonal Δ_Q on $Q_*\hat{\mathcal{A}}$. In turn, Δ_Q induces a non-coassociative diagonal Δ_C on $C_*\hat{\mathcal{A}}$ via p and q .

Given a generator $(D, f, g, \omega) \in Q_*\hat{\mathcal{A}}$ and a subset $X \subseteq \{e_1, \dots, e_k\} = g^{-1}(m)$, let $\bar{X} = g^{-1}(m) \setminus X$ and $\rho(X) = \#\{(e_i, e_j) \in X \times \bar{X} \mid i < j\}$. Consider the following related generators:

- $(D/X, f, g_{D/X}, \omega_{D/X})$, where D/X is obtained from D by contracting the edges of X , $g_{D/X}$ is the labeling induced by g , and $\omega_{D/X}$ is the orientation obtained from ω by deleting all factors in X ;
- $(D_{\bar{X}}, f, g_{D_{\bar{X}}}, \omega_{D_{\bar{X}}})$, where $D_{\bar{X}}$ is obtained from D by reversing labels on the edges in \bar{X} , $g_{D_{\bar{X}}}$ agrees with g except on \bar{X} , and $\omega_{D_{\bar{X}}}$ is the orientation obtained from ω by deleting all factors in \bar{X} .

Definition 5.1. Define $\Delta_Q : Q_*\hat{\mathcal{A}} \rightarrow Q_*\hat{\mathcal{A}} \otimes Q_*\hat{\mathcal{A}}$ on generators by

$$\Delta_Q(D, f, g, \omega) = \sum_{X \subseteq g^{-1}(m)} (-1)^{\rho(X)} (D/X, f, g_{D/X}, \omega_{D/X}) \otimes (D_{\bar{X}}, f, g_{D_{\bar{X}}}, \omega_{D_{\bar{X}}}).$$

In particular, if c is a corolla, then $\Delta_Q(c, f, g, 1) = (c, f, g, 1) \otimes (c, f, g, 1)$, where g is the empty map.

The restriction of Δ_Q to the submodule \mathcal{A}_∞ generated by metric planar rooted trees defines a (strictly coassociative) DG coalgebra structure on \mathcal{A}_∞ that commutes with the operadic structure, see [MS, Proposition 5.1].

Definition 5.2. Define $\Delta_C : C_*\hat{\mathcal{A}} \rightarrow C_*\hat{\mathcal{A}} \otimes C_*\hat{\mathcal{A}}$ to be the composition

$$C_*\hat{\mathcal{A}} \xrightarrow{q} Q_*\hat{\mathcal{A}} \xrightarrow{\Delta_Q} Q_*\hat{\mathcal{A}} \otimes Q_*\hat{\mathcal{A}} \xrightarrow{p \otimes p} C_*\hat{\mathcal{A}} \otimes C_*\hat{\mathcal{A}}.$$

To simplify notation, we sometimes abuse notation and write $D \in C_*\hat{\mathcal{A}}_y^{\mathbf{x}}$ when we mean (D, f, ω_D) .

Proposition 5.3. *On a corolla $(c, f, +1) \in C_k\hat{\mathcal{A}}_y^{\mathbf{x}}$ we have*

$$\Delta_C(c, f, +1) = \sum_{\substack{S \otimes T \in C_i\hat{\mathcal{A}}_y^{\mathbf{x}} \otimes C_j\hat{\mathcal{A}}_y^{\mathbf{x}} \\ S_{\max} \leq T_{\min} \\ i+j=k}} \pm (S, f, \omega_S) \otimes (T, f, \omega_T).$$

Proof. We evaluate the composition $(p \otimes p) \circ \Delta_Q \circ q$:

$$\begin{aligned} \Delta_C(c, f, +1) &= (p \otimes p)\Delta_Q(q(c, f, +1)) \\ &= \sum_{B \in C_0\hat{\mathcal{A}}_y^{\mathbf{x}}} (p \otimes p)\Delta_Q(B, f, m, \omega_B^{\text{std}}) \\ &= \sum_{\substack{B \in C_0\hat{\mathcal{A}}_y^{\mathbf{x}} \\ X \subseteq \mathcal{E}(B)}} \pm p(B/X, f, g_{B/X}, \omega_{B/X}) \otimes p(B_{\bar{X}}, f, g_{B_{\bar{X}}}, \omega_{B_{\bar{X}}}). \end{aligned}$$

To evaluate $p(B_{\bar{X}}, f, g_{B_{\bar{X}}}, \omega_{B_{\bar{X}}})$, note that the non-metric edges of the binary diagram B are exactly the edges in $\bar{X} = \{e_1, \dots, e_{k-1}\}$, and B decomposes as a

\circ_i -composition of fully metric binary diagrams B_1, \dots, B_k along the edges of \bar{X} :

$$(B_{\bar{X}}, f, g_{B_{\bar{X}}}, \omega_{B_{\bar{X}}}) = \pm \sigma \cdot [(B_1, f_1, m, \omega_1) \circ_{e_1} \cdots \circ_{e_{k-1}} (B_k, f_k, m, \omega_k)]$$

(such decompositions are unique up to operadic associativity). Since B_i is fully metric, Lemma 4.5 implies that $p(B_i, f_i, m, \omega_i)$ is a corolla if B_i is maximal and vanishes otherwise. Hence if $p(B_{\bar{X}}, f, g_{B_{\bar{X}}}, \omega_{B_{\bar{X}}}) \neq 0$, each B_i is maximal and $p(B_{\bar{X}}, f, g_{B_{\bar{X}}}, \omega_{B_{\bar{X}}}) = \pm (B/X, f, \omega_{B/X})$. Furthermore, if $(T, f, \omega_T) \in C_* \hat{\mathcal{A}}_y^x$, there is a unique B with maximal B_i 's such that $T = B/X$. Consequently,

$$\begin{aligned} \Delta_C(c, f, 1) &= \sum_{\substack{B \in C_0 \hat{\mathcal{A}}_y^x \\ X \subseteq \mathcal{E}(B) \\ \text{all } B_i \text{ maximal}}} \pm p(B/X, f, g_{B/X}, \omega_{B/X}) \otimes (B/X, f, \omega_{B/X}) \\ &= \sum_{\substack{S \otimes T \in C_i \hat{\mathcal{A}}_y^x \otimes C_j \hat{\mathcal{A}}_y^x \\ S_{\max} \leq T_{\min} \\ i+j=k}} \pm (S, f, \omega_S) \otimes (T, f, \omega_T). \end{aligned}$$

□

Remark 5.4. In [MS, Proposition 5.1], Markl and Shnider proved the special case of Proposition 5.3 with Δ_C restricted to the submodule \mathcal{A}_∞ generated by planar rooted trees. Since Δ_Q is induced by the Serre diagonal on T^n , it is strictly coassociative on $Q_* \hat{\mathcal{A}}$. However, Δ_C is not coassociative. In fact, Markl and Shnider also remarked that Δ_C cannot be chosen to be coassociative on \mathcal{A}_∞ . Nevertheless, this structure is homotopy coassociative, and the formula for Δ_C in Proposition 5.3 extends to a A_∞ -coalgebra structure on $C_* \hat{\mathcal{A}}$ in a natural way (for the special \mathcal{A}_∞ case see [L]).

6. COMPUTATIONS

In this section, we make explicit computations and remarks about the diagonal Δ_C in various situations. In Example 6.1 we calculate the diagonal of $I_{2,0}$, in Example 6.2 we make some general remarks about the diagonal of a cyclic A_∞ -algebra, and in Remark 6.3 we comment on the diagonal for strong homotopy inner products in the sense of [C]. In all of these considerations, we ignore signs and always write “+” regardless of orientation.

Example 6.1. To evaluate $\Delta_C = (p \otimes p) \circ \Delta_Q \circ q$ on the corolla $I_{2,0}$, note that

$$q(I_{2,0}) = \begin{array}{c} \diagdown \quad \diagup \\ \bullet \\ \diagup \quad \diagdown \\ m \quad m \end{array} + \begin{array}{c} \diagup \quad \diagdown \\ \bullet \\ \diagdown \quad \diagup \\ m \quad m \end{array} + \begin{array}{c} \diagdown \quad \diagup \\ \bullet \\ \diagdown \quad \diagup \\ m \quad m \end{array} + \begin{array}{c} \diagup \quad \diagdown \\ \bullet \\ \diagup \quad \diagdown \\ m \quad m \end{array} + \begin{array}{c} \diagdown \quad \diagup \\ \bullet \\ \diagdown \quad \diagup \\ m \quad m \end{array}$$

is the sum of the five squares in the metric pairahedron pictured in Figure 4. Evaluating the Serre diagonal on each of these squares gives

$$\begin{aligned} \Delta_Q \left(\begin{array}{c} \diagdown \quad \diagup \\ \bullet \\ \diagup \quad \diagdown \\ m \quad m \end{array} + \begin{array}{c} \diagup \quad \diagdown \\ \bullet \\ \diagdown \quad \diagup \\ m \quad m \end{array} + \begin{array}{c} \diagdown \quad \diagup \\ \bullet \\ \diagdown \quad \diagup \\ m \quad m \end{array} + \begin{array}{c} \diagup \quad \diagdown \\ \bullet \\ \diagup \quad \diagdown \\ m \quad m \end{array} + \begin{array}{c} \diagdown \quad \diagup \\ \bullet \\ \diagdown \quad \diagup \\ m \quad m \end{array} \right) = \\ \begin{array}{c} \begin{array}{c} \diagup \quad \diagdown \\ \bullet \\ \diagdown \quad \diagup \\ m \quad m \end{array} \otimes \begin{array}{c} \diagdown \quad \diagup \\ \bullet \\ \diagup \quad \diagdown \\ m \quad m \end{array} + \begin{array}{c} \diagdown \quad \diagup \\ \bullet \\ \diagdown \quad \diagup \\ m \quad m \end{array} \otimes \begin{array}{c} \diagup \quad \diagdown \\ \bullet \\ \diagdown \quad \diagup \\ n \quad n \end{array} + \begin{array}{c} \diagup \quad \diagdown \\ \bullet \\ \diagdown \quad \diagup \\ m \quad m \end{array} \otimes \begin{array}{c} \diagdown \quad \diagup \\ \bullet \\ \diagup \quad \diagdown \\ m \quad m \end{array} + \begin{array}{c} \diagdown \quad \diagup \\ \bullet \\ \diagdown \quad \diagup \\ m \quad m \end{array} \otimes \begin{array}{c} \diagup \quad \diagdown \\ \bullet \\ \diagdown \quad \diagup \\ n \quad n \end{array} \\ + \begin{array}{c} \diagup \quad \diagdown \\ \bullet \\ \diagdown \quad \diagup \\ m \quad m \end{array} \otimes \begin{array}{c} \diagdown \quad \diagup \\ \bullet \\ \diagdown \quad \diagup \\ m \quad m \end{array} + \begin{array}{c} \diagdown \quad \diagup \\ \bullet \\ \diagdown \quad \diagup \\ m \quad m \end{array} \otimes \begin{array}{c} \diagup \quad \diagdown \\ \bullet \\ \diagdown \quad \diagup \\ n \quad n \end{array} + \begin{array}{c} \diagup \quad \diagdown \\ \bullet \\ \diagdown \quad \diagup \\ m \quad m \end{array} \otimes \begin{array}{c} \diagdown \quad \diagup \\ \bullet \\ \diagdown \quad \diagup \\ m \quad m \end{array} \\ + \begin{array}{c} \diagdown \quad \diagup \\ \bullet \\ \diagdown \quad \diagup \\ m \quad m \end{array} \otimes \begin{array}{c} \diagup \quad \diagdown \\ \bullet \\ \diagdown \quad \diagup \\ m \quad m \end{array} + \begin{array}{c} \diagdown \quad \diagup \\ \bullet \\ \diagdown \quad \diagup \\ m \quad m \end{array} \otimes \begin{array}{c} \diagup \quad \diagdown \\ \bullet \\ \diagdown \quad \diagup \\ n \quad n \end{array} + \begin{array}{c} \diagup \quad \diagdown \\ \bullet \\ \diagdown \quad \diagup \\ m \quad m \end{array} \otimes \begin{array}{c} \diagdown \quad \diagup \\ \bullet \\ \diagdown \quad \diagup \\ m \quad m \end{array} \end{array}$$

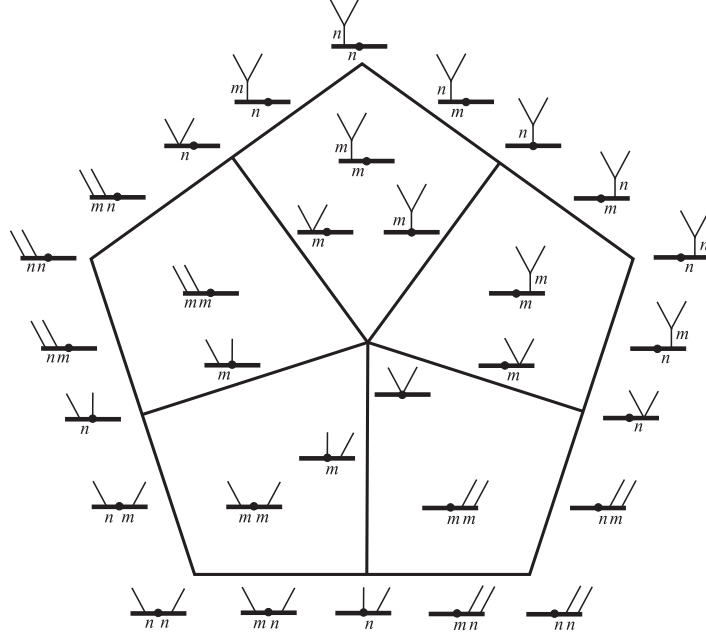


FIGURE 4. The metric pairahedron associated with $I_{2,0}$ (metric edges m vary in length; non-metric edges n have fixed length 1).

$$\begin{aligned}
 & + \begin{array}{c} \diagup \\ \bullet \\ \diagdown \end{array} \otimes \begin{array}{c} \diagup \\ \bullet \\ \diagdown \end{array} + \begin{array}{c} \diagup \\ \bullet \\ \diagdown \end{array} \otimes \begin{array}{c} \diagup \\ \bullet \\ \diagdown \end{array} + \begin{array}{c} \diagup \\ \bullet \\ \diagdown \end{array} \otimes \begin{array}{c} \diagup \\ \bullet \\ \diagdown \end{array} + \begin{array}{c} \diagup \\ \bullet \\ \diagdown \end{array} \otimes \begin{array}{c} \diagup \\ \bullet \\ \diagdown \end{array} + \begin{array}{c} \diagup \\ \bullet \\ \diagdown \end{array} \otimes \begin{array}{c} \diagup \\ \bullet \\ \diagdown \end{array} \\
 & + \begin{array}{c} \diagup \\ \bullet \\ \diagdown \end{array} \otimes \begin{array}{c} \diagup \\ \bullet \\ \diagdown \end{array} + \begin{array}{c} \diagup \\ \bullet \\ \diagdown \end{array} \otimes \begin{array}{c} \diagup \\ \bullet \\ \diagdown \end{array} + \begin{array}{c} \diagup \\ \bullet \\ \diagdown \end{array} \otimes \begin{array}{c} \diagup \\ \bullet \\ \diagdown \end{array} + \begin{array}{c} \diagup \\ \bullet \\ \diagdown \end{array} \otimes \begin{array}{c} \diagup \\ \bullet \\ \diagdown \end{array} + \begin{array}{c} \diagup \\ \bullet \\ \diagdown \end{array} \otimes \begin{array}{c} \diagup \\ \bullet \\ \diagdown \end{array}.
 \end{aligned}$$

All terms above lie in the kernel of $p \otimes p$ except

$$\begin{array}{c} \diagup \\ \bullet \\ \diagdown \end{array} \otimes \begin{array}{c} \diagup \\ \bullet \\ \diagdown \end{array} + \begin{array}{c} \diagup \\ \bullet \\ \diagdown \end{array} \otimes \begin{array}{c} \diagup \\ \bullet \\ \diagdown \end{array} + \begin{array}{c} \diagup \\ \bullet \\ \diagdown \end{array} \otimes \begin{array}{c} \diagup \\ \bullet \\ \diagdown \end{array} + \begin{array}{c} \diagup \\ \bullet \\ \diagdown \end{array} \otimes \begin{array}{c} \diagup \\ \bullet \\ \diagdown \end{array} + \begin{array}{c} \diagup \\ \bullet \\ \diagdown \end{array} \otimes \begin{array}{c} \diagup \\ \bullet \\ \diagdown \end{array} + \begin{array}{c} \diagup \\ \bullet \\ \diagdown \end{array} \otimes \begin{array}{c} \diagup \\ \bullet \\ \diagdown \end{array}.$$

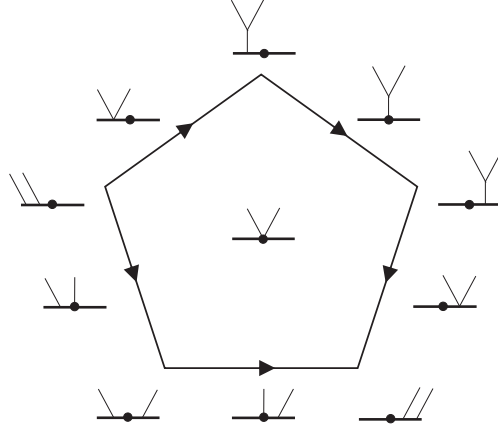
Applying $p \otimes p$ we obtain

$$\begin{aligned}
 \Delta_C \left(\begin{array}{c} \diagup \\ \bullet \\ \diagdown \end{array} \right) &= \begin{array}{c} \diagup \\ \bullet \\ \diagdown \end{array} \otimes \begin{array}{c} \diagup \\ \bullet \\ \diagdown \end{array} + \begin{array}{c} \diagup \\ \bullet \\ \diagdown \end{array} \otimes \begin{array}{c} \diagup \\ \bullet \\ \diagdown \end{array} + \begin{array}{c} \diagup \\ \bullet \\ \diagdown \end{array} \otimes \begin{array}{c} \diagup \\ \bullet \\ \diagdown \end{array} \\
 &+ \begin{array}{c} \diagup \\ \bullet \\ \diagdown \end{array} \otimes \begin{array}{c} \diagup \\ \bullet \\ \diagdown \end{array} + \left(\begin{array}{c} \diagup \\ \bullet \\ \diagdown \end{array} + \begin{array}{c} \diagup \\ \bullet \\ \diagdown \end{array} \right) \otimes \begin{array}{c} \diagup \\ \bullet \\ \diagdown \end{array}.
 \end{aligned}$$

Note that if D is a right-factor in a non-primitive term of $\Delta_C(I_{2,0})$, the set of all left-hand factors that pair off with D in $\Delta_C(I_{2,0})$ form a path from the minimal vertex of $I_{2,0}$ to the maximal vertex of $I_{2,0}$ (see Figure 5).

Example 6.2. Let us calculate Δ_C in low dimensions in the setting of a *cyclic* A_∞ -algebra. In this case, the corolla $I_{k,l} = 0$ whenever $k + l > 0$, and the non-trivial inner product $I_{0,0}$ consists of two thick horizontal edges joined at a common vertex. Thus we compute $\Delta_C(c) = \sum \pm S \otimes T$ by summing over all diagrams for inner products S and T such that $S_{\max} \leq T_{\min}$ (see Proposition 5.3). This gives:

$$\Delta_C(I_{0,0}) = I_{0,0} \otimes I_{0,0},$$

FIGURE 5. The vertex poset of $I_{2,0}$.

$$\begin{aligned}\Delta_C(I_{1,0}) &= \Delta_C(I_{0,1}) = \Delta_C(I_{1,1}) = 0, \\ \Delta_C(I_{2,0}) &= \text{---}\blacktriangledown\text{---} \otimes \text{---}\blacktriangledown\text{---}.\end{aligned}$$

Note that $\Delta_C(I_{2,0})$ corresponds to the homotopy $\varrho_{2,0}$ mentioned in the Introduction. The above expression is a special case of the following more general formula:

$$\Delta_C(I_{k,l}) = \sum_{r=0}^{k+l} \sum_{i=1}^{p_r} S_i^{(r)} \otimes T_i^{(k+l-r)},$$

where $S_i^{(q)}, T_i^{(q)} \in C_q \hat{\mathcal{A}}$ are of degree q . In the special case of cyclic A_∞ -algebras, the $r=0$ and $r=k+l$ terms vanish, and the $r=1$ and $r=k+l-1$ terms are given by the formula:

$$\begin{aligned}\Delta_C(I_{k,l}) &= \text{---}\bigvee\text{---} \otimes \left(\text{---}\blacktriangledown\text{---} + \text{---}\blacktriangledown\text{---} + \cdots + \text{---}\blacktriangledown\text{---} \right) \\ &+ \text{---}\bigvee\text{---} \otimes \left(\text{---}\blacktriangledown\text{---} + \text{---}\blacktriangledown\text{---} + \cdots + \text{---}\blacktriangledown\text{---} \right) \\ &+ \sum_{r=2}^{k+l-2} \sum_i S_i^{(r)} \otimes T_i^{(k+l-r)} \\ &+ \left(\text{---}\blacktriangledown\text{---} + \text{---}\blacktriangledown\text{---} + \cdots + \text{---}\blacktriangledown\text{---} \right) \otimes \text{---}\bigvee\text{---} \\ &+ \left(\text{---}\blacktriangledown\text{---} + \text{---}\blacktriangledown\text{---} + \cdots + \text{---}\blacktriangledown\text{---} \right) \otimes \text{---}\bigvee\text{---}.\end{aligned}$$

Computing Δ_C in general requires more work, as the formula for $\Delta_C(I_{4,0})$ shows:

$$\Delta_C(I_{2,1}) = \text{---}\blacktriangledown\text{---} \otimes \text{---}\blacktriangledown\text{---} + \text{---}\blacktriangledown\text{---} \otimes \text{---}\blacktriangledown\text{---},$$

$$\begin{aligned}
 \Delta_C(I_{3,0}) &= \begin{array}{c} \Downarrow \\ \bullet \\ \hline \end{array} \otimes \left(\begin{array}{c} \Downarrow \\ \bullet \\ \hline \end{array} + \begin{array}{c} \Downarrow \\ \bullet \\ \hline \end{array} \right) \\
 &+ \left(\begin{array}{c} \Downarrow \\ \bullet \\ \hline \end{array} + \begin{array}{c} \Downarrow \\ \bullet \\ \hline \end{array} \right) \otimes \begin{array}{c} \Downarrow \\ \bullet \\ \hline \end{array}, \\
 \Delta_C(I_{4,0}) &= \begin{array}{c} \Downarrow \\ \bullet \\ \hline \end{array} \otimes \left(\begin{array}{c} \Downarrow \\ \bullet \\ \hline \end{array} + \begin{array}{c} \Downarrow \\ \bullet \\ \hline \end{array} + \begin{array}{c} \Downarrow \\ \bullet \\ \hline \end{array} \right) \\
 &+ \begin{array}{c} \Downarrow \\ \bullet \\ \hline \end{array} \otimes \begin{array}{c} \Downarrow \\ \bullet \\ \hline \end{array} + \begin{array}{c} \Downarrow \\ \bullet \\ \hline \end{array} \otimes \begin{array}{c} \Downarrow \\ \bullet \\ \hline \end{array} \\
 &+ \begin{array}{c} \Downarrow \\ \bullet \\ \hline \end{array} \otimes \begin{array}{c} \Downarrow \\ \bullet \\ \hline \end{array} + \begin{array}{c} \Downarrow \\ \bullet \\ \hline \end{array} \otimes \begin{array}{c} \Downarrow \\ \bullet \\ \hline \end{array} \\
 &+ \left(\begin{array}{c} \Downarrow \\ \bullet \\ \hline \end{array} + \begin{array}{c} \Downarrow \\ \bullet \\ \hline \end{array} + \begin{array}{c} \Downarrow \\ \bullet \\ \hline \end{array} \right) \otimes \begin{array}{c} \Downarrow \\ \bullet \\ \hline \end{array}
 \end{aligned}$$

Remark 6.3. In Example 6.2 we observed that the tensor product of cyclic A_∞ -algebras is, in general, not cyclic. One could also consider strong homotopy inner products considered by Cho [C], which are cyclic A_∞ -algebras up to homotopy, and ask whether or not the tensor product preserves such structures. In [C, Theorem 5.1], Cho showed that a homotopy inner product transforms into a strong homotopy inner product if and only if it satisfies the following three conditions:

- (1) Skew Symmetry: $I_{k,l}(a, \underline{b}, c, \underline{d}) = \pm I_{l,k}(c, \underline{d}, a, \underline{b})$,
- (2) Closedness:

$$\begin{aligned}
 I_{k+l+1,m}(\dots, a, \dots, \underline{b}, \dots, \underline{c}) \pm I_{k,l+m+1}(\dots, \underline{a}, \dots, b, \dots, \underline{c}) \\
 \pm I_{l+m+1,k}(\dots, c, \dots, \underline{a}, \dots, \underline{b}) = 0,
 \end{aligned}$$

- (3) Homological non-degeneracy: $(I_{0,0})_*$ is non-degenerate.

For more details on the notation and signs, we refer the reader to [C] or [T2]. Now the symmetrical nature of the definition of Δ_C implies that the tensor product of two skew-symmetric homotopy inner products (satisfying condition (1)) is also skew-symmetric: If S^* denotes the diagram obtained from S by rotating 180° , then $(S^*)_{\max} = (S_{\max})^*$, $(D^*)_{\min} = (D_{\min})^*$, and $S_{\max} \leq D_{\min} \Leftrightarrow (S_{\max})^* \leq (D_{\min})^*$. Furthermore, under reasonable conditions, it is clear that the tensor product of two homologically non-degenerate homotopy inner products (satisfying property (3)) is also homologically non-degenerate. Thus we conjecture that tensor products also preserve property (2), and that the tensor product is closed in the strong homotopy inner product category.

Acknowledgments. We wish to thank Jean-Louis Loday and Jim Stasheff for sharing their thoughts and insights with us during discussions related to this topic.

APPENDIX A. SIGNS

In this appendix we discuss various issues related to the definition and calculation of signs in this paper. To begin, we review the signs in an A_∞ -algebra with homotopy inner products, define the canonical orientation of a binary diagram, and check the signs in Proposition 3.2.

A.1. Signs in an A_∞ -algebra with homotopy inner product. Let $A = \bigoplus_{i \in \mathbb{Z}} A_i$ be a differential graded R -module (DGM) with differential $d : A \rightarrow A$ of degree $+1$. The tensor product of DGM maps f and g satisfies $(f \otimes g)(a \otimes b) = (-1)^{|g| \cdot |a|} f(a) \otimes g(b)$. If $(A^1, d^1), \dots, (A^{k+1}, d^{k+1})$ are DGMs, the induced differential d on $A^1 \otimes \dots \otimes A^k$ is given by

$$d = \sum_{i=1}^k \mathbf{1}^{\otimes i-1} \otimes d^i \otimes \mathbf{1}^{\otimes k-i},$$

and the induced differential D on $\text{Hom}(A^1 \otimes \dots \otimes A^k, A^{k+1})$ is given by the commutator

$$[D, f] = d^{k+1} f - (-1)^{|f|} f d.$$

An A_∞ -algebra structure on A consists of a family of maps $\{\mu_k : A^{\otimes k} \rightarrow A\}_{k \geq 2}$ such that $|\mu_k| = 2 - k$ and

$$(A.1) \quad [D, \mu_k] = \sum_{j+\ell=k+1} \sum_{i=1}^{k-j+1} (-1)^{i(j+1)+j\ell} \mu_\ell \left(\mathbf{1}^{\otimes(i-1)} \otimes \mu_j \otimes \mathbf{1}^{\otimes(k-j-i+1)} \right).$$

Remark A.1. There are various choices of signs in the A_∞ -algebra structure relations. For example, one could define an A_∞ -algebras in terms of maps $\mu'_k : A^{\otimes k} \rightarrow A$ such that

$$[d, \mu'_k] = \sum_{j+\ell-1=k} \sum_{i=1}^{k-j+1} (-1)^{(i-1) \cdot (j+1) + \ell} \cdot \mu'_\ell \circ \left(\underbrace{\mathbf{1} \otimes \dots \otimes \mathbf{1}}_{i-1 \text{ factors}} \otimes \mu'_j \otimes \underbrace{\mathbf{1} \otimes \dots \otimes \mathbf{1}}_{k-j-i+1 \text{ factors}} \right).$$

The two definitions are related via the relation $\mu'_k = (-1)^{\frac{k(k+1)}{2}+1} \cdot \mu_k$. Note that the simplest signs arise by shifting dimension in A up by 1 and removing all signs. We refer the reader *e.g.* to [T1] and [SU] for details.

An ∞ -bimodule over A consists of a DGM M together with a family of module maps $\{\lambda_{j', j''} : A^{\otimes j'} \otimes M \otimes A^{\otimes j''} \rightarrow M\}$ such that

$$(A.2) \quad [D, \lambda_{k', k''}] = \sum_{j+\ell=k+1} \sum_{i=1}^{k-j+1} (-1)^{i(j+1)+j\ell} \lambda_{\ell', \ell''} \left(\mathbf{1}^{\otimes(i-1)} \otimes q_J \otimes \mathbf{1}^{\otimes(k-j-i+1)} \right),$$

where $k = k' + k'' + 1$, $\ell = \ell' + \ell'' + 1$, and q_J is either $\lambda_{j', j''}$ or μ_j , which is determined by the i^{th} to the $(k-j+i)^{\text{th}}$ input in $A^{\otimes k'} \otimes M \otimes A^{\otimes k''}$. An important example of an ∞ -bimodule is given by setting $M = A$ and $\lambda_{j', j''} = \mu_{j'+j''+1}$. This will help to clarify the signs in the formula above.

Finally, given ∞ -bimodule over A , a *homotopy inner product* consists of a family of maps $\{\varrho_{j', j''} : M \otimes A^{\otimes j'} \otimes M \otimes A^{\otimes j''} \rightarrow R\}$, such that

$$(A.3) \quad [D, \varrho_{k', k''}] = \sum_{j'+j''+\ell=k} (-1)^{(j+1)+j\ell+j'(j''+\ell)} \varrho_{\ell', \ell''} \left(\lambda_{j', j''} \otimes \mathbf{1}^{\otimes(k-j'-j''-1)} \right) \underbrace{(\tau_{\#} \circ \dots \circ \tau_{\#})}_{j' \text{ cyclic permut.}} \\ + \sum_{j+\ell-1=k} \sum_{i=2}^{k-j+1} (-1)^{i(j+1)+j\ell} \varrho_{\ell', \ell''} \left(\mathbf{1}^{\otimes(i-1)} \otimes q_J \otimes \mathbf{1}^{\otimes(k-j-i+1)} \right),$$

where $k = k' + k'' + 2$, $\ell = \ell' + \ell'' + 2$, and q_J is either $\lambda_{j', j''}$ or μ_j depending on the inputs. The first line of the fomula involves composition in the first position ($i = 1$) after cyclically permuting j' elements from back-to-front, i.e.,

$$\tau_{\#} : A^{\otimes i'} \otimes M \otimes A^{\otimes i''} \otimes M \otimes A^{\otimes i'''+1} \rightarrow A^{\otimes i'+1} \otimes M \otimes A^{\otimes i''} \otimes M \otimes A^{\otimes i'''},$$

then applying $\lambda_{j', j''}$. This cyclical rotation of j' elements gives rise to the additional sign coefficient here.

The signs (A.1), (A.2), and (A.3), which appear in the definitions of an A_∞ -algebra and a homotopy inner product, also appear in the definition of $C_*\hat{\mathcal{A}}$. Let $\mathcal{E}nd_{(A, M, R)}$ denote the endomorphism operad of the triple (A, M, R) . Then under the conventions above, a morphism of operads $C_*\hat{\mathcal{A}} \rightarrow \mathcal{E}nd_{(A, M, R)}$ defines an A_∞ -algebra A with homotopy inner product structure on M , as is evident in the next definition.

Definition A.2. Given an A_∞ -algebra with ∞ -bimodule and homotopy inner product structures $(A, M, R, \{\mu_i\}_i, \{\lambda_{i,j}\}_{i,j}, \{\varrho_{i,j}\}_{i,j})$, define the operad map $F : C_*\hat{\mathcal{A}} \rightarrow \mathcal{E}nd_{(A, M, R)}$ as follows: For a corolla $c = T_i, M_{i,j}$ or $I_{i,j}$ (see Figure 1), the canonical clockwise assignment f_\circ of inputs (see Figure 3), and the canonical orientation $\omega = +1$ of the empty set of edges, define $F(c, f_\circ, +1)$ to be the structure associated with this corolla, i.e.,

$$F(T_i, f_\circ, +1) = \mu_i, \quad F(M_{i,j}, f_\circ, +1) = \lambda_{i,j}, \quad F(I_{i,j}, f_\circ, +1) = \varrho_{i,j}.$$

For a diagram D with exactly one edge e and the canonical clockwise indexing f_\circ , the signs in F are determined by (A.1), (A.2), and (A.3). For example, if $D \in C_*\hat{\mathcal{A}}_1^{11\cdots 1}$ is a tree and the edge $e = e(i, j)$ determines the subtree T_j attached to T_ℓ at position i , then, from (A.1),

$$F(D, f_\circ, e(i, j)) = d_{e(i, j)}(\mu_k) := (-1)^{i(j+1)+j\ell} \mu_\ell(1^{\otimes i-1} \otimes \mu_j \otimes 1^{\otimes \ell-i}).$$

Similarly, for a general diagram D and any edge $e \in \mathcal{E}(D)$, we have an operation d_e of degree $+1$, and set

$$F(D, f_\circ, e_1 \wedge \cdots \wedge e_r) = d_{e_1} \circ \cdots \circ d_{e_r}(q_J),$$

where q_J is one of the maps $\mu_i, \lambda_{i,j}$, or $\varrho_{i,j}$. When d_e passes a structure map $q'_{J'}$, the usual Koszul sign commutation rule applies: $d_e \circ q'_{J'} = (-1)^{|q'_{J'}|} q'_{J'} \circ d_e$.

Finally, for a non-trivial labeling $f : \{1, \dots, k\} \rightarrow \mathcal{L}(D)$, we uniquely write f as a composition of a permutation $\sigma \in S_k$ and the clockwise labeling, $f = f_\circ \circ \sigma$, and denoting by $\sigma_{\#}(x_1 \otimes \cdots \otimes x_k) = x_{\sigma^{-1}(1)} \otimes \cdots \otimes x_{\sigma^{-1}(k)}$ a permutation of tensor factors, we set

$$F(D, f_\circ \circ \sigma, \omega) = \text{sgn}(\sigma) \cdot F(D, f_\circ, \omega) \circ \sigma_{\#}.$$

With this, one can check that the signs appearing in Equation (2.1) make F into an operad map. For example, for $(D, f_\circ, \omega_D) \in C_n\hat{\mathcal{A}}_1^{11\cdots 1}$, $k = \#\mathcal{L}(D)$, and $(E, id, \omega_E) \in C_m\hat{\mathcal{A}}_1^{11\cdots 1}$, $l = \#\mathcal{L}(E)$, we have

$$\begin{aligned} & F((D, f_\circ, e_1^D \wedge \cdots \wedge e_{k-n-2}^D) \circ_i (E, f_\circ, e_1^E \wedge \cdots \wedge e_{l-m-2}^E)) \\ &= (-1)^{km+i(l+1)} F(D \circ_i E, f_\circ, e_1^D \wedge \cdots \wedge e_{k-n-2}^D \wedge e_1^E \wedge \cdots \wedge e_{l-m-2}^E \wedge e) \\ &= (-1)^{km+i(l+1)} d_{e_1^D} \circ \cdots \circ d_{e_{k-n-2}^D} \circ d_{e_1^E} \circ \cdots \circ d_{e_{l-m-2}^E} \circ d_e(\mu_{k+l-1}) \\ &= (-1)^{k(m+l)} d_{e_1^D} \circ \cdots \circ d_{e_{k-n-2}^D} \circ d_{e_1^E} \circ \cdots \circ d_{e_{l-m-2}^E}(\mu_k \circ (1^{\otimes i-1} \otimes \mu_l \otimes 1^{\otimes l-j})) \end{aligned}$$

$$\begin{aligned}
&= d_{e_1^D} \circ \cdots \circ d_{e_{k-n-2}^D} (\mu_k \circ (1^{\otimes i-1} \otimes d_{e_1^E} \circ \cdots \circ d_{e_{l-m-2}^E} (\mu_l) \otimes 1^{\otimes l-j})) \\
&= F(D, f_{\cup}, e_1^D \wedge \cdots \wedge e_{k-n-2}^D) \circ_i F(E, f_{\cup}, e_1^E \wedge \cdots \wedge e_{l-m-2}^E).
\end{aligned}$$

A similar calculation applies in the other cases.

A.2. Orientation on binary trees. In this appendix, we describe the canonical orientation of a binary diagram, either as element of $C_*\hat{\mathcal{A}}$ or as a non-metric element of $Q_*\hat{\mathcal{A}}$. The main ingredient is an extension of Mac Lane’s Coherence Theorem [MacL] to homotopy inner products, by which any two paths of binary diagrams are connected via sequences of pentagons, hexagons, and squares.

Definition A.3. A **path of binary diagrams** is a sequence of binary diagrams $\beta = (B_1, \dots, B_n)$ such that (B_i, B_{i+1}) is an edge-pair for all i (see Definition 4.1).

We consider paths up to equivalence, where the equivalence relation is generated by,

$$(\dots, B_{i-1}, B_i, B_{i+1}, \dots) \sim (\dots, B_{i-1}, B_i, \tilde{B}_i, B_i, B_{i+1}, \dots),$$

where \tilde{B}_i is related to B_i by a local move.

For example, the boundaries of the pentagons $T_4, M_{0,3}, M_{1,2}, M_{2,1}, M_{3,0}, I_{2,0}, I_{0,2}$ and the hexagon $I_{1,1}$ are paths for any choice of starting/ending point. Furthermore, two disjoint local moves define a square path (called a *naturality square*) by applying move 1, then move 2, then undoing move 1, and undoing move 2. A *fundamental path* is a naturality square or the boundary paths of one of the aforementioned corollas.

Definition A.4. Two (equivalence classes of) paths are **one-step-connected** if they differ (locally) by a fundamental path. Two paths β_1 and β_m are **connected** if there is a sequence of paths β_1, \dots, β_m such that β_i and β_{i+1} are one-step-connected for all i .

For example, consider a diagram P_1 and a sequence of diagrams $(P_1, P_2, P_3, P_4, P_5, P_1)$ that differ locally from P_1 by a fundamental path, which is the boundary of the Stasheff pentagon. Then the following paths β_1 and β_2 are one-step-connected: $\beta_1 = (B_1, \dots, B_{k-1}, P_1, B_{k+1}, \dots, B_n)$ and $\beta_2 = (B_1, \dots, B_{k-1}, P_1, P_2, P_3, P_4, P_5, P_1, B_{k+1}, \dots, B_n)$.

Lemma A.5 (Coherence Lemma). *Any two paths $\beta = (B_1, \dots, B_n)$ and $\beta' = (B'_1, \dots, B'_{n'})$ such that $B_1 = B'_1$ and $B_n = B'_{n'}$ are connected.*

The lemma can be proved in the same manner as the “associative Coherence Lemma” in [MacL, Section VII.2.]. Thus to define a concept on binary diagrams via paths, it is sufficient to check that the definition is independent of path with respect to fundamental paths. Let us do this for the notion of the standard orientation next. First note that each local move from $B \rightsquigarrow B'$ (as given by (1)-(6) in Definition 4.1 with its induced identification of edges) transfers an orientation ω from B to B' by setting $\omega = e_1 \wedge \cdots \wedge e_k = -\omega'$. One can check that traversing any of the fundamental paths preserves orientation (see Figure 6 for example).

Thus if $\beta = (B, \dots, B')$ is a path from diagram B to diagram B' , an orientation ω on B transfers to an orientation ω_β on B' . And furthermore, Lemma A.5 assures us that ω_β is independent of path since it is preserved along paths coming from fundamental paths. Let us use this idea to define the standard orientation ω_B^{std} on a binary diagram B .

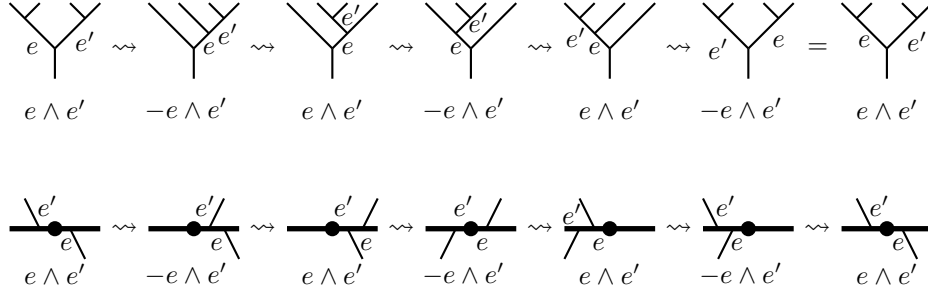


FIGURE 6. Orientation is preserved along boundaries of corollas T_4 (top line) and $I_{1,1}$ (bottom line).

Definition A.6. Let B be a binary diagram of the three types pictured in Figure 7. Define the **standard orientation** ω_B^{std} on B by

$$\omega_B^{\text{std}} := e_1 \wedge \cdots \wedge e_k \in \bigwedge^k \mathcal{E}(B)$$

The standard orientation on a general binary diagram B is induced by any path from one of the diagrams in Figure 7 to B .

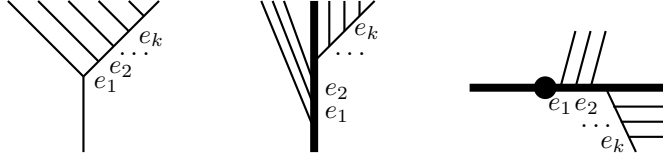


FIGURE 7. Diagrams with standard orientation $e_1 \wedge \cdots \wedge e_k$

Our last task in this subsection is to define the orientation $\omega(S, D)$ that is needed in the definition of the morphism p for a generator $(D, f_\cup, m, \omega_D) \in Q_k \hat{\mathcal{A}}$ of degree k , and a diagram S with $S_{\max} \leq D_{\min}$. This will be done in four steps: First, we define the orientation ξ_B for binary diagrams B , second, we define the contraction $\omega \rfloor \xi_B$, third, we define notion of positive and negative edges and show how they are relevant for p , and fourth we use the notion of positive and negative edges to find the orientation $\omega(S, D)$ on S by contracting $\omega \rfloor \xi_{S_{\max}}$ for some ω .

Step 1. Following [MS], we first define the orientation

$$\xi_B := (-1)^{\frac{(n-2)(n-3)}{2}} \cdot \omega_B^{\text{std}} = (-1)^{1+2+\cdots+(n-3)} \cdot \omega_B^{\text{std}}$$

for a binary diagram B with standard orientation ω_B^{std} , n leaves, and $n - 2$ edges.

Remark A.7. There is an alternative description of ξ_B given in [MS]. For this, first define $\xi_B = +1$ for the binary diagrams B in $C_0 \hat{\mathcal{A}}$ with 2 leaves and no edges (*i.e.* $B = T_2, M_{1,0}, M_{0,1}$, or $I_{0,0}$). Then for a general binary diagram B , the orientation ξ_B is determined by the composition relation in $C_0 \hat{\mathcal{A}}$,

$$(B' \circ_{f_\cup(i)} B'', f_\cup, \xi_{B' \circ_{f_\cup(i)} B''}) = \sigma \cdot ((B', f_\cup, \xi_{B'}) \circ_i (B'', f_\cup, \xi_{B''})).$$

This can derive this formula by comparing ξ_B for two binary diagrams related by one of the local moves from Definition A.3.

Step 2. If B is a binary tree with orientation ω , and ω' is an orientation on a subset of edges of B , then define $\omega']\omega$ by the relation $\langle e', e \rangle = \delta_{e', e} \in \{0, 1\}$, where $\delta_{e', e}$ denotes the Kronecker delta. In particular, if $\omega = e_1 \wedge \cdots \wedge e_r \wedge e_{r+1} \wedge \cdots \wedge e_k$ and $\omega' = e_1 \wedge \cdots \wedge e_r$, then

$$\omega']\omega = (-1)^{\frac{r(r-1)}{2}} \cdot e_{r+1} \wedge \cdots \wedge e_k.$$

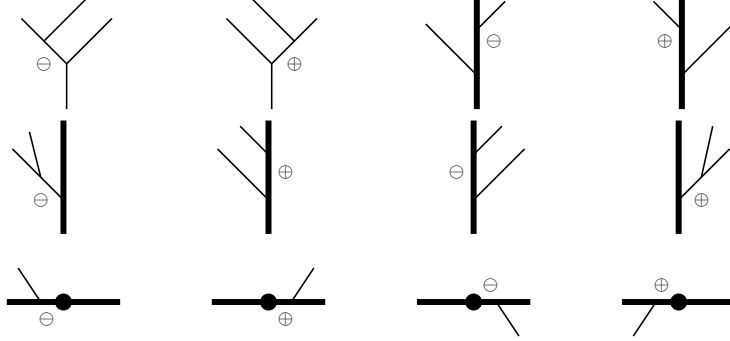
Now, if $S_{\max} = D_{\min}$, then as we shall see in Step 3, $S = D_{\min}/\{\text{edges in } D\}$, in which case we define $\omega(S, D) = \omega_D']\xi_{D_{\min}}$. Now, consider a corolla c for example. Since $1]\omega = \omega$ and $\omega_B^{\text{std}}]\xi_B = +1$, we obtain

$$(A.4) \quad S = c_{\min}, D = c, \omega_D = 1 \Rightarrow \omega(S, D) = 1]\xi_{c_{\min}} = \xi_{c_{\min}},$$

$$(A.5) \quad S = c, D = c_{\max}, \omega_D = \omega_{c_{\max}}^{\text{std}} \Rightarrow \omega(S, D) = \omega_{c_{\max}}^{\text{std}}]\xi_{c_{\max}} = +1.$$

Step 3. To further analyze the condition $S_{\max} \leq D_{\min}$ we need to introduce the notion of positive and negative edges in a binary diagram. Markl and Shnider ([MS]) refer to these notions as left-leaning and right-leaning, respectively.

Definition A.8. Let B be a binary diagram. We define an edge to be positive, denoted by \oplus , respectively negative, denoted by \ominus , if it appears in B in the following way,



We denote the number of positive edges in a binary diagram B by $|B|_{\oplus}$.

Lemma A.9. *Positive and negative edges have the following properties:*

- (1) *If $B \leq B'$, then $|B|_{\oplus} \leq |B'|_{\oplus}$, i.e., $|\cdot|_{\oplus}$ preserves the order. The maximal (resp. minimal) binary diagram c_{\max} (resp. c_{\min}) of a corolla c given by Lemma 4.2 is the unique diagram all of whose edges are positive (resp. negative).*
- (2) *If S is a diagram, then $S = S_{\max}/\{e_1, \dots, e_r\}$ is a quotient in which only positive edges of S_{\max} are collapsed. If D is a diagram, then $D = D_{\min}/\{e_1, \dots, e_s\}$ is a quotient in which only negative edges of D_{\min} are collapsed.*
- (3) *Let $(D, f_{\circlearrowleft}, m, \omega_D) \in Q_k \hat{\mathcal{A}}$. If $|D_{\min}|_{\oplus} \neq k$, then $p(D, f_{\circlearrowleft}, m, \omega_D) = 0$. If $|D_{\min}|_{\oplus} = k$, then $D = D_{\min}/\{\text{negative edges}\}$, and if $(S, f, \omega) \in C_k \hat{\mathcal{A}}$ is a summand of $p(D, f_{\circlearrowleft}, m, \omega_D)$, then S_{\max} has exactly k positive edges and $S = S_{\max}/\{\text{positive edges}\}$.*

Proof.

- (1) This can be checked by direct inspection.
- (2) For a diagram S , we obtain S_{\max} by inserting positive edges at every non-binary vertex. For a diagram D , we obtain D_{\min} by inserting negative edges at every non-binary vertex.
- (3) Since D has k edges and D_{\min} is obtained from D by inserting only negative edges, D_{\min} has at most k positive edges. If $(S, f, \omega) \in C_k \hat{\mathcal{A}}$, then S_{\max} is obtained from S by inserting k positive edges; consequently S_{\max} has at least k positive edges. Since $S_{\max} \leq D_{\min}$, we have $k \leq |S_{\max}|_{\oplus} \leq |D_{\min}|_{\oplus} \leq k$. Therefore S_{\max} and D_{\min} must have exactly k positive edges. Furthermore, the k positive edges in D_{\min} are exactly the ones coming from D , and the k positive edges in S_{\max} are exactly the ones inserted in S . \square

Step 4. Now, let $(D, f_{\circlearrowleft}, m, \omega_D) \in Q_k \hat{\mathcal{A}}$ be a generator of degree k , and let S be a diagram with $S_{\max} \leq D_{\min}$. In order to define $\omega(S, D)$, we may assume by Lemma A.9 (3), that exactly k edges e_1, \dots, e_k of D_{\min} are positive, and these are the edges of D , *i.e.*, $\omega_D = \eta \cdot e_1 \wedge \dots \wedge e_k$ for some $\eta \in \{+1, -1\}$.

We can now define $\omega(S, D)$ in the general case.

Definition A.10. If $S_{\max} = D_{\min}$, then $S = D_{\min}/\{e_1, \dots, e_k\}$, and we set $\omega(S, D) := \omega_D \rfloor \xi_{D_{\min}}$ as in step 2. If $S_{\max} < D_{\min}$, then $S = S_{\max}/\{\text{positive edges}\}$ by Lemma A.9 (3), and we set $\omega(S, D) := (\eta \cdot e_1 \wedge \dots \wedge e_k) \rfloor \xi_{S_{\max}}$, where the positive edges in D_{\min} and S_{\max} are identified using the local moves from Definition A.3. The ambiguity of identifying positive edges under paths is given (according to the Coherence Lemma A.5) by pentagons, hexagons and squares. Since the pentagons and hexagons change the number of positive edges, changing a path $\beta = (D_{\min}, \dots, S_{\max})$ to another path $\beta' = (D_{\min}, \dots, S_{\max})$ only consists of squares, for which the positive edges remain identified uniquely. (Note, that for a local move $B \rightsquigarrow B'$ from Definition A.3 with constant number of positive edges, the procedure of keeping track of the positive edge by renaming a positive edge e_{\oplus} by one negative edge e_{\ominus} gives $\dots \wedge e_{\ominus} \wedge \dots \wedge e_{\oplus} \wedge \dots = -\dots \wedge e_{\oplus} \wedge \dots \wedge e_{\ominus} \wedge \dots$, which is the induced orientation $\xi_{B'}$ on B' .)

A.3. Sign check for Proposition 3.2. We now give the remaining sign details for Proposition 3.2. More precisely, in the notation of the proof of Proposition 3.2, we will show that $(-1)^{i+1} \omega_B^{\hat{e}_i}$ equals $(-1)^{\epsilon_2} \omega_j$.

We calculate $(-1)^{\epsilon_2} \omega_j$ of the binary diagram B from the proof of Proposition 3.2 and compare it to $\omega_B^{\hat{e}_i}$. Recall that B is a composition of B' and B'' with standard orientations corresponding to c' and c'' with $(-1)^{\epsilon_1} \cdot \sigma \cdot ((c', f_{\circlearrowleft}, 1) \circ_j (c'', f'_{\circlearrowleft}, 1)) = (D', f'_{\circlearrowleft}, e')$ and $D'/e' = c$. If the corolla c' has r leaves and the corolla c'' has s leaves, then the original corolla c has $k = r + s - 1$ leaves. Hence, from the definition of the composition in Equation (2.1), and of the S_k action, we see that $(-1)^{\epsilon_1} = \text{sgn}(\sigma) \cdot (-1)^{j \cdot (s+1) + r \cdot s}$. Furthermore, from the definition of the composition in $Q_* \hat{\mathcal{A}}$, we have $\omega_j = \omega_{B'}^{\text{std}} \wedge \omega_{B''}^{\text{std}}$. The only other signs come from comparing ω_j to ω_B^{std} , and a possible application of σ . We consider two cases: Case 1: $\sigma = id_k$. Case 2: $\sigma \neq id_k$.

Case 1: Either the corolla c is *not* an inner product diagram, or c is an inner product diagram and the composition \circ_j is *not* on the thick left module input.

Case 2: The corolla c is an inner product diagram and the composition \circ_j is on the thick left module input.

In Case 1, the only way to obtain $(c, f_{\circ}, 1)$ as a composition of c' and c'' is via the canonical labelings f_{\circ} for c' and c'' and $\sigma = id$. In this case, the proof follows as in [MS, Proposition 4.2]. More precisely, with the notation from the left diagram

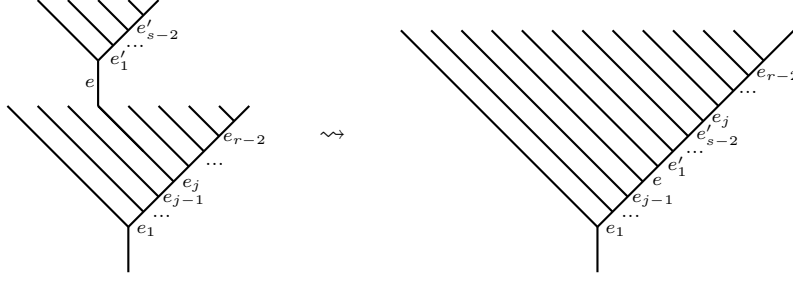


FIGURE 8. Move the edges e, e'_1, \dots, e'_{s-2} to the right.

in Figure 8, we have

$$\begin{aligned} (-1)^{\epsilon_2} \omega_j &= (-1)^{j(s+1)+rs} \cdot e_1 \wedge \cdots \wedge e_{r-2} \wedge e'_1 \wedge \cdots \wedge e'_{s-2} \\ &= (-1)^{j+s} \cdot e_1 \wedge \cdots \wedge e_{j-1} \wedge e'_1 \wedge \cdots \wedge e'_{s-2} \wedge e_j \wedge \cdots \wedge e_{r-2}. \end{aligned}$$

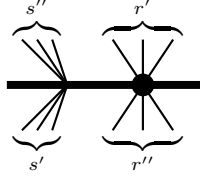
On the other hand, the standard orientation for the left diagram in Figure 8 is $\omega_B^{\text{std}} = (-1)^{s-1} \cdot e_1 \wedge \cdots \wedge e_{j-1} \wedge e \wedge e'_1 \wedge \cdots \wedge e'_{s-2} \wedge e_j \wedge \cdots \wedge e_{r-2}$, which can be seen via the $(s-1)$ local moves to the diagram on the right in Figure 8. Setting $i = j$, we obtain,

$$(-1)^{i+1} \omega_B^{\hat{e}} = (-1)^{j+s} \cdot e_1 \wedge \cdots \wedge e_{j-1} \wedge e'_1 \wedge \cdots \wedge e'_{s-2} \wedge e_j \wedge \cdots \wedge e_{r-2} = (-1)^{\epsilon_2} \omega_j.$$

The considerations in other types of diagrams for Case 1 are similar to the one in Figure 8.

Now, for Case 2, where $c' = I_{r', r''}$ is an inner product corolla and $c'' = M_{s', s''}$ is a module tree, with $r = r' + r'' + 2$ and $s = s' + s'' + 1$, we have

$$(I_{r', r''}, f_{\circ}, 1) \circ_1 (M_{s', s''}, f_{\circ}, 1) = (-1)^{(s+1)+r \cdot s} \cdot (I_{r'+s'', r''+s'}, f_{\circ} \circ \tau^{s'}, 1),$$



where $\tau \in \mathbb{Z}_k \subset S_k$ is the cyclic rotation “ $-1 \pmod k$ ”. Thus, $\sigma = \tau^{s'}$ with $\text{sgn}(\sigma) = (-1)^{s' \cdot (r+s'')}$, and thus $(-1)^{\epsilon_1} = (-1)^{s+1+rs+s'(r+s'')}$. Similarly to before, we obtain (see Figure 9)

$$(-1)^{\epsilon_2} \omega_1 = (-1)^{s+1+rs+s'(r+s'')} \cdot e_1 \wedge \cdots \wedge e_{r-2} \wedge e'_1 \wedge \cdots \wedge e'_{s-2}.$$

On the other hand, the standard orientation of the left diagram in Figure 9 is

$$\begin{aligned} \omega_B^{\text{std}} &= (-1)^{s-1+r} \cdot e'_{s'} \wedge \cdots \wedge e_{s'+s''-1} \wedge e \wedge e_1 \wedge \cdots \wedge e_{r-2} \wedge e'_1 \wedge \cdots \wedge e'_{s'-1} \\ &= (-1)^{s-1+r+s''(r+s')} \cdot e \wedge e_1 \wedge \cdots \wedge e_{r-2} \wedge e'_1 \wedge \cdots \wedge e'_{s'-1} \wedge e'_{s'} \wedge \cdots \wedge e'_{s-2}, \end{aligned}$$

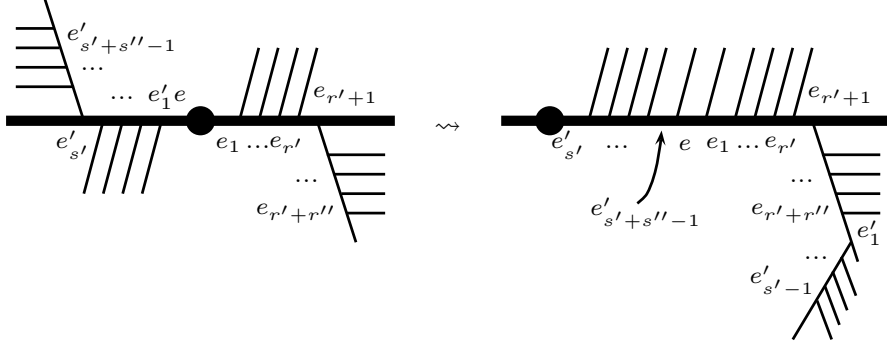


FIGURE 9. The edges on the left are brought to the right in $(s + r - 3)$ moves: $s' - 1$ to move $e'_1, \dots, e'_{s'}$ on one branch; 2 to move the obtained two main branches from left to right; $r' + r''$ to move the “ s'' ”-branch all the way to the right; and $s'' - 1$ to move the edges from the “ s'' ”-branch to the thick right edge.

which can be seen by performing $(s + r - 3)$ local moves yielding the right diagram in Figure 9. Thus for $i = 1$, we obtain

$$(-1)^{i+1} \cdot \omega_B^e = (-1)^{s+r-3+s''(r+s')} \cdot e_1 \wedge \dots \wedge e_{r-2} \wedge e'_1 \wedge \dots \wedge e'_{s-2} = (-1)^{\varepsilon_2} \cdot \omega_1,$$

where we used the fact that $s = s' + s'' + 1$, so that $(-1)^{r+s''r} = (-1)^{rs+s'r}$.

This completes the check of both cases, and with this also the proof of Proposition 3.2.

APPENDIX B. PROOF OF PROPOSITION 3.3 (CONTRACTIBILITY OF T_n , $M_{k,l}$, AND $I_{k,l}$)

In this appendix, we prove Proposition 3.3: *The polytopes associated with T_n , $M_{k,l}$, and $I_{k,l}$ are contractible.*

First, recall that Stasheff proved in [S, Proposition 3], that the associahedra T_n are contractible. Furthermore the cell complexes for $M_{k,n-k}$, $I_{n,0}$ and $I_{0,n}$ are isomorphic to the one for T_n . It remains to check the case $I_{k,l}$ with $k, l \geq 1$, which will be proved by showing that the polyhedron associated with $I_{k,l}$ for $k, l \geq 1$ is homeomorphic to a $(k + l)$ -ball, and thus contractible. To this end, we derive an analog of Stasheff’s result.

To outline the idea, we fix natural numbers k and l , and set $n = k + l$. We will show that the boundary of $I_{k,l}$ is an $(n - 1)$ -sphere by identifying it with two $(n - 1)$ -disks that are glued along an $(n - 2)$ -sphere. The two $(n - 1)$ -disks, which we denote by $\overline{I_{k,l}^{up}}$ and $\overline{I_{k,l}^{low}}$, are (roughly) the respective components of the boundary of $I_{k,l}$ given by expanding edges in the upper and the lower part of $I_{k,l}$, cf. Definition B.2. The intersection $\overline{I_{k,l}^{up}} \cap \overline{I_{k,l}^{low}}$ consists of diagrams, that have at least one upper and one lower edge expanded. The core of the proof consists of identifying this intersection with an $(n - 2)$ -sphere. Recall that Stasheff [S, Section 6] represented the associahedron K_{n+2} as a subdivision of a cube. We construct a convenient bijection between $\overline{I_{k,l}^{up}}$ and those boundary components of the associahedron indexed by 2 to $(k + 2)$, see also Figure 13 on page 27.

We start by defining the boundary components $\overline{I_{k,l}^{up}}$ and $\overline{I_{k,l}^{low}}$, and show how these are related to the associahedron K_{n+2} . For this, we first index the internal edges of a diagram as specified in Definition B.1.

Definition B.1. Label the incoming external edges of $I_{k,l}$ and K_{n+2} from 1 to $k+l+2$ in a clockwise manner, starting from the furthest left (see Figure 10). For

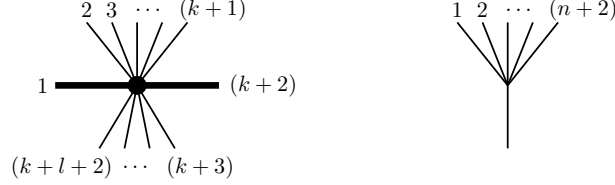


FIGURE 10. The canonical labeling of the leaves

each diagram in the boundary of $I_{k,l}$ and K_{n+2} , label the incoming external edges by the same rule. If e is an internal edge of $I_{k,l}$ or K_{n+2} , assign to e the smallest number of all incoming edges above e . An interior edge in $I_{k,l}$ that is labeled by an element of $\{2, \dots, k+2\}$ will be called an upper edge, whereas an interior edge labeled by an element of $\{1, k+3, \dots, k+l+2\}$ will be called a lower edge.

For example, all internal edges of the diagrams in Figure 11 are labeled according to the rule in Definition B.1. Furthermore, in the left diagram of Figure 11, an

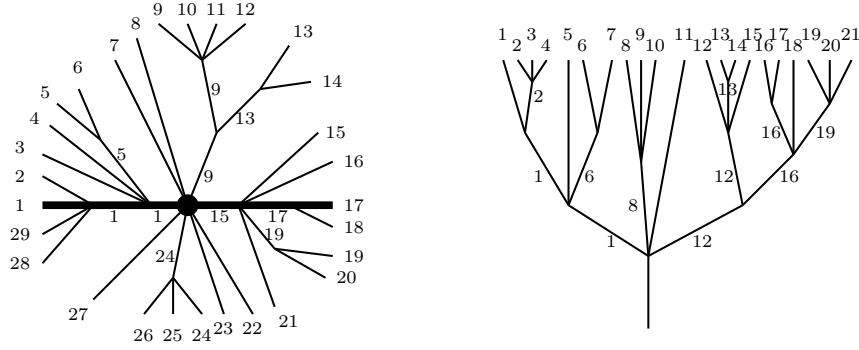


FIGURE 11. The labeling of internal edges

edge labeled by an element of $\{2, \dots, 17\}$ is an upper edge, and an edge labeled by $\{1, 18, \dots, 29\}$ is a lower edge.

Note, that contracting an interior edge does not change the labels of other interior edges, because a label only depends on the incoming edges above it. Consequently, the boundary ∂ of a diagram, which is defined by summing over all possible ways of expanding an edge, also preserves this labeling.

Definition B.2. For a subset $X \subset \{1, \dots, k+l+2\}$, we denote by $I_{k,l}^X$ (respectively K_{n+2}^X) the space generated by all diagrams that are given by edge insertions of $I_{k,l}$

(respectively K_{n+2}), such that all internal edges are labeled by numbers in X . For example, the diagrams displayed in Figure 11 are diagrams in $I_{15,12}^{\{1,5,9,13,15,17,19,24\}}$ and in $K_{21}^{\{1,2,6,8,12,13,16,19\}}$, respectively. It is important to note that in the special case of $X = \{2, \dots, k+2\}$, there is a bijection between $I_{k,l}^X$ and K_{n+2}^X . This correspondence is given by attaching (or detaching) the outgoing edge between the external edges $k+l+2$ and the 1, as depicted in Figure 12.

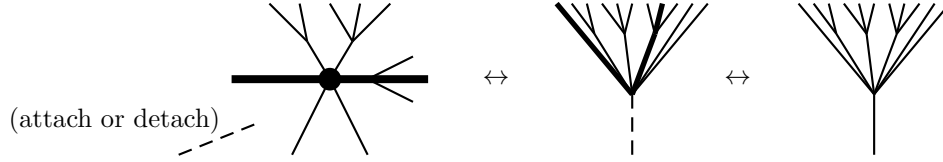


FIGURE 12. Attaching an edge to $I_{k,l}$ below the left thick edge, or detaching the outgoing edge in K_{n+2}

We denote by $I_{k,l}^{up} := I_{k,l}^{\{2, \dots, k+2\}}$ the module generated by diagrams that have only upper interior edges. Similarly, $I_{k,l}^{low} := I_{k,l}^{\{1, k+3, \dots, k+l+2\}}$ is the module generated by diagrams that have only lower interior edges. Furthermore, we denote by $\overline{I_{k,l}^{up}}$ the module generated by diagrams, that have at least one upper edge, and by $\overline{I_{k,l}^{low}}$ the module generated by diagrams, that have at least one lower edge. Generators in $I_{k,l}^{up}$ are called upper diagrams, whereas those in $I_{k,l}^{low}$ are called lower diagrams.

Let $C_*(\overline{I_{k,l}})$ be the dg-module generated by all edge insertions of $I_{k,l}$, then $I_{k,l}^{up}$, $I_{k,l}^{low}$, $\overline{I_{k,l}^{up}}$, and $\overline{I_{k,l}^{low}}$ are submodules of $C_*(\overline{I_{k,l}})$. In fact, $\overline{I_{k,l}^{up}}$ and $\overline{I_{k,l}^{low}}$ are subcomplexes of $C_*(\overline{I_{k,l}})$, which are the closures of $I_{k,l}^{up}$ and $I_{k,l}^{low}$, respectively.

With the notions of upper and lower edges, we are now ready to prove Proposition 3.3.

Proof of Proposition 3.3. We will show that $C_*(\overline{I_{k,l}})$ can be realized as a polyhedron whose boundary is homeomorphic to a $(k+l-1)$ -sphere. Note that the case $k+l=1$ is trivial. Inductively, assume this has been shown for all $I_{k',l'}$ with $k'+l' < k+l$.

Note that the boundary of $C_*(\overline{I_{k,l}})$ consists of upper diagrams (elements of $I_{k,l}^{up}$), lower diagrams (elements of $I_{k,l}^{low}$), and diagrams that have both upper and lower edges (elements of $\overline{I_{k,l}^{up}} \cap \overline{I_{k,l}^{low}}$). The proof now follows in three steps:

- Step 1: The realizations of both $I_{k,l}^{up}$ and $I_{k,l}^{low}$ are homeomorphic to open $(k+l-1)$ -disks.
- Step 2: The subcomplexes $\overline{I_{k,l}^{up}}$ and $\overline{I_{k,l}^{low}}$ of $C_*(\overline{I_{k,l}})$ are realized by closed $(k+l-1)$ -disks.
- Step 3: The intersection $\overline{I_{k,l}^{up}} \cap \overline{I_{k,l}^{low}}$ is realized by a $(k+l-2)$ -sphere.

The claim then follows from steps 2 and 3, since the boundary of $C_*(\overline{I_{k,l}})$ is realized by two $(k+l-1)$ -disks glued together along a $(k+l-2)$ -sphere. \square

Proof of step 1. Definition B.2 establishes a one-to-one correspondence between diagrams in $I_{k,l}^{up}$ and $K_{n+2}^{\{2,\dots,k+2\}}$. Since this correspondence is boundary preserving, it defines a correspondence between their realizations. Now in [S, Section 6], Stasheff gives an explicit realization of $K_{n+2}^{\{2,\dots,k+2\}}$ as an open $(n-1)$ -ball on the boundary of the n -cube $[0, 1]^n$. More precisely, denote the coordinates of $[0, 1]^n$ by (t_1, \dots, t_n) . Then $K_{n+2}^{\{2,\dots,k+2\}}$ is realized on those boundaries of $[0, 1]^n$ with $t_2 = 1$, or $t_3 = 1$, \dots , or $t_{k+2} = 1$. This proves the claim for $I_{k,l}^{up}$.

To identify $I_{k,l}^{low}$ with $K_{n+2}^{\{2,\dots,l+2\}}$, relabel the exterior edges of $I_{k,l}$ by assigning “1” to the right-most edge, and continuing in a clockwise direction. Note, that edges previously labeled by $k+3, \dots, k+l+2$ or 1, are now, under the new labeling, labeled by $2, \dots, l+2$, respectively. Repeating the argument above shows that $I_{k,l}^{low}$ is also realized as an open $(n-1)$ -ball. \square

Proof of step 2. Lemma B.3 below shows that the homeomorphism of the realizations of $I_{k,l}^{up}$ and $K_{n+2}^{\{2,\dots,k+2\}}$ extend to their closures in the realizations of $I_{k,l}$ and K_{n+2} , respectively. Since the closure $\overline{K_{n+2}^{\{2,\dots,k+1\}}}$ is realized in [S, Section 6] as a closed $(n-1)$ -ball, this holds for $\overline{I_{k,l}^{up}}$ as well. The statement for $\overline{I_{k,l}^{low}}$ then follows as in step 1, by relabeling the external edges, starting with “1” at the right-most external edge. \square

Proof of step 3. Since $\overline{I_{k,l}^{up}}$ is a closed $(k+l-1)$ -ball with interior $I_{k,l}^{up}$, the boundary of $\overline{I_{k,l}^{up}}$ is realized as a $(k+l-2)$ -sphere. Now, the boundary of $\overline{I_{k,l}^{up}}$ is $\overline{I_{k,l}^{up}} - I_{k,l}^{up} = \overline{I_{k,l}^{up}} \cap \overline{I_{k,l}^{low}}$, i.e., the boundary of the space of diagrams having only upper edges consists of all diagrams that have at least one upper and one lower edge. Thus $\overline{I_{k,l}^{up}} \cap \overline{I_{k,l}^{low}}$ is a $(k+l-2)$ -sphere. \square

Lemma B.3. *The homeomorphism of the realizations of $I_{k,l}^{up}$ and $K_{n+2}^{\{2,\dots,k+2\}}$ extends to the closure $\overline{I_{k,l}^{up}}$ and $\overline{K_{n+2}^{\{2,\dots,k+2\}}}$ (in $I_{k,l}$ and K_{n+2} , respectively).*

Proof. By step 1, we know that $I_{k,l}^{up}$ and $K_{n+2}^{\{2,\dots,k+2\}}$ are isomorphic modules, and Stasheff has shown in [S, Section 6] that $\overline{K_{n+2}^{\{2,\dots,k+2\}}}$ can be realized as a closed $(n-1)$ -ball \bar{B}_{n-1} where $K_{n+2}^{\{2,\dots,k+2\}}$ are the cells in the interior of the $(n-1)$ -ball. For example, for $I_{2,1}^{up}$ and $K_5^{\{2,3,4\}}$, this is shown in Figure 13.

In a similar way we wish to realize the closure $\overline{I_{k,l}^{up}}$ in a similar way as a closed $(n-1)$ -ball \bar{B}_{n-1} . Since $I_{k,l}^{up}$ and $K_{n+2}^{\{2,\dots,k+2\}}$ are isomorphic modules, we may choose the same cells for the interior of the ball \bar{B}_{n-1} that were chosen for $K_{n+2}^{\{2,\dots,k+2\}}$ and identify them with the diagrams of $I_{k,l}^{up}$. We need to find cells on the boundary of \bar{B}_{n-1} that correspond to the boundary of $\overline{I_{k,l}^{up}}$. We will do this for the closure $\bar{\alpha}$ of each cell α in the interior B_{n-1} and we will see from the construction that this induces a well-defined cell subdivision realizing $\overline{I_{k,l}^{up}}$.

First, if the closure $\bar{\alpha}$ of α lies completely inside the interior B_{n-1} then the boundary of α is already completely given by corresponding cells. Thus, we may assume that α has a boundary piece that lies on the boundary of \bar{B}_{n-1} . We choose the cell subdivision by induction on the dimension of the cell α . If α is an edge

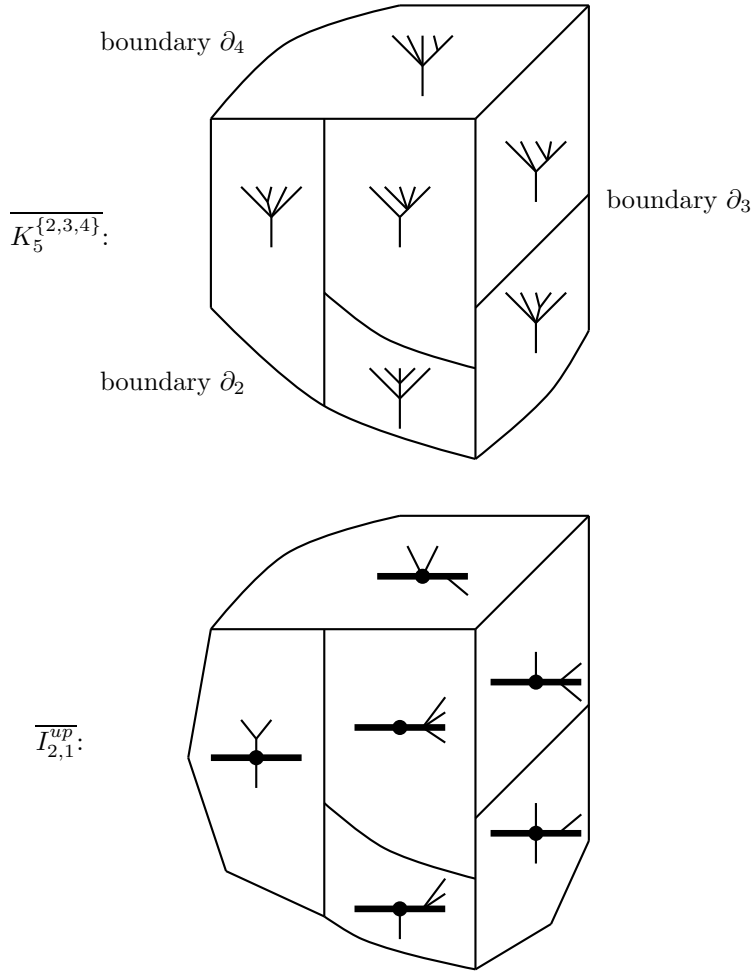


FIGURE 13. Identification between $I_{2,1}^{up}$ and $K_5^{\{2,3,4\}}$ (see also [S, Figure 18])

and corresponds to a diagram $D \in I_{k,l}^{up}$, then all vertices are binary except one, which is ternary, and the boundary vertices are identified with the boundary of the diagram D in $\overline{I_{k,l}^{up}}$. Now, let α be a cell of the open $(n-1)$ -ball B_{n-1} of dimension s , which corresponds to a diagram D in $I_{k,l}^{up}$. By induction we assume that for all cells α' of B_{n-1} of dimension $< s$ that correspond to a diagram D' , we have already chosen a cell subdivision of the closure $\overline{\alpha'}$ realizing the closure of D' . Thus, we already have our cell subdivision for $\overline{\partial\alpha \cap B_{n-1}}$. Since α also corresponds to a diagram in $K_{n+2}^{\{2,\dots,k+1\}}$, we know that $\overline{\alpha}$ is a closed s -ball, and that $\overline{\partial\alpha \cap B_{n-1}}$ is a closed $(s-1)$ -ball. Since D is a diagram of lower degree than $I_{k,l}$, we may use the induction hypothesis of the proposition to see that the realization of D is a Cartesian product of lower dimensional balls, which is again homeomorphic to an

s -ball. The cells of $\overline{\partial\alpha \cap B_{n-1}}$ realize some boundary pieces of D as a closed $(s-1)$ -ball on the boundary of $\bar{\alpha}$. Consequently, we may complete this cell subdivision to all of $\bar{\alpha}$, and with this give a realization of the closure of D .

Thus, we have constructed a cell subdivision of \bar{B}_{n-1} such that for each cell α corresponding to a diagram D of $I_{k,l}^{up}$, the closure of α realizes the complex generated by D . Furthermore this construction is natural in the sense that if α' is in the boundary of α , then, by construction, the cells of $\bar{\alpha}'$ are also cells of $\bar{\alpha}$. Combining these cells for all of \bar{B}_{n-1} , we obtain a cell subdivision such that every point of \bar{B}_{n-1} lies in exactly one cell. (This is clear for the open ball B_{n-1} , and every point of $\partial\bar{B}_{n-1}$ lies in the boundary of some cell α of B_{n-1} so that the naturality condition guarantees uniqueness.) Furthermore there is a bijective correspondence between cells of $\overline{I_{k,l}^{up}}$ and those in \bar{B}_{n-1} , which realizes $\overline{I_{k,l}^{up}}$ as a closed $(n-1)$ -ball. To see this, note that the assignment of diagrams from $\overline{I_{k,l}^{up}}$ to cells of \bar{B}_{n-1} is surjective by construction, and respects the boundary, since it does so locally for each closed cell. We also claim that two diagrams D_1 and D_2 that correspond to the same cell in \bar{B}_{n-1} must be equal. To see this, consider the cell α in \bar{B}_{n-1} corresponding to D_1 and D_2 , then α is in the boundary of a unique smallest dimensional cell α' in the interior B_{n-1} . Denote by D' the diagram corresponding to α' . Now, D_1 itself is in the boundary of some diagram D'' in the interior $I_{k,l}^{up}$, and we denote by α'' the cell corresponding to D'' . Since D_1 is in the boundary of D'' , α must be in the boundary of α'' . Since α' is the lowest dimensional cell containing α , α' must be in the boundary of α'' or equal to it. Since B_{n-1} realizes $I_{k,l}^{up}$, it must also be that D' is in the boundary of D'' or equal to it. In any case, since D'' is realized by α'' , we see that D_1 is in the boundary of D' . A similar argument shows that D_2 is also in the boundary of D' . Again, using that D' is realized by α' , we see that there is only one diagram $D_1 = D_2$ corresponding to the cell α . Therefore $\overline{I_{k,l}^{up}}$ is realized by a cell decomposition of \bar{B}_{n-1} .

This completes the proof of the lemma. \square

APPENDIX C. PROOF THAT “ \leq ” IS A PARTIAL ORDER

In this appendix, we show that the relation defined Definition 4.1 induces a well-defined partial ordering on binary diagrams. For diagrams $C_*\hat{\mathcal{A}}_y^{\mathbf{x}}$ with a coloring $\mathbf{x} = (1, \dots, 1), y = 1$, this is a well-known fact known as the Tamari partial order, see [Ta]. We will extend this to binary diagrams in $C_*\hat{\mathcal{A}}$ of all colors.

It is sufficient to prove antisymmetry: $D = D'$ whenever $D \leq D'$ and $D' \leq D$. For a module diagram $D \in C_*\hat{\mathcal{A}}_y^{\mathbf{x}}$ of coloring $\mathbf{x} = (1, \dots, 2, \dots, 1), y = 2$ let $\ell(D)$ (respectively $r(D)$) be the number of edges attached to the thick vertical edge coming from the left (respectively from the right), see Figure 14. Note that ℓ and r respect the order in the sense, if $D \leq D'$ then $\ell(D) \leq \ell(D')$ and $r(D) \geq r(D')$. Now, consider an edge e of D that is attached to the thick vertical edge from the right, and let $u(e)$ denote the number of edges that are attached to the thick edge from the left and that lie above e . Define $u(D) = \sum_e u(e)$, where the sum is taken over all edges e that are attached to the thick edge from the right (see Figure 14). Note, that relation (1) from Definition 4.1 leaves u invariant, whereas (2) preserves the order, *i.e.*, if $D < D'$ via the relation (2) then $u(D) < u(D')$.

Now, let $D, D' \in C_*\hat{\mathcal{A}}_y^{\mathbf{x}}$ with $\mathbf{x} = (1, \dots, 2, \dots, 1), y = 2$. If $D \leq D'$ and $D' \leq D$ then we have $\ell(D) = \ell(D')$ and $r(D) = r(D')$. Since relation (3) strictly increases

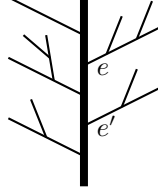


FIGURE 14. An example with $\ell(D) = 3$, $r(D) = 2$, $u(e) = 1$,
 $u(e') = 2$, $u(D) = 1 + 2 = 3$

ℓ and relation (4) strictly decreases r , only relations (1) and (2) can be applied to generate $D \leq D'$ and $D' \leq D$. Furthermore, since (2) strictly increases u , we obtain that $u(D) = u(D')$, and only relation (1) can be applied. Using the known fact that (1) is a partial order implies the claim $D = D'$ for module diagrams $D, D' \in C_*\hat{\mathcal{A}}_y^{\mathbf{x}}$.

Finally, for inner product diagrams $D \in C_*\hat{\mathcal{A}}_y^{\mathbf{x}}$ with $\mathbf{x} = (1, \dots, 2, \dots, 2, \dots, 1)$, $y = 0$, let $tl(D)$ (resp. $bl(D)$, $tr(D)$, $br(D)$) be the number of edges attached to the top of the thick horizontal edge and left of the the thick vertex (resp. bottom left, top right, and bottom right), see Figure 15. For $D \leq D'$, we have that

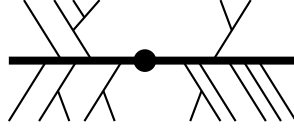


FIGURE 15. An example with $tl(D) = 2$, $bl(D) = 3$, $tr(D) = 1$,
 and $br(D) = 5$

$tl(D) \geq tl(D')$, $bl(D) \leq bl(D')$, $tr(D) \leq tr(D')$, and $br(D) \geq br(D')$. Thus, for $D \leq D'$ and $D' \leq D$, all of tl , bl , tr , and br coincide on D and D' . Since relations (3)-(6) change at least one of tl , bl , tr , or br , these cannot be applied to generate $D \leq D'$ and $D' \leq D$. To finish the proof, we refer back to the case of the module diagram with $\mathbf{x} = (1, \dots, 2, \dots, 1)$, $y = 2$, using the function u and the Tamari partial ordering as before to see that $D = D'$.

APPENDIX D. PROOF OF PROPOSITION 4.6 (p IS A CHAIN MAP)

In this appendix, we proof that $p : Q_*\hat{\mathcal{A}} \rightarrow C_*\hat{\mathcal{A}}$ is a chain map. The proof is an extension of Markl and Shnider's proof of Proposition 4.6 in [MS] and uses the notion of positive or negative edges in a binary inner product diagram as defined in Definition A.8 in Appendix A.2. The maximal binary diagrams is the one with only positive edges, and the minimal binary diagram is the one with only negative edges. (In [MS] these edges were called left and of right leaning edges, respectively.) The main part of the proof amounts to checking that for $(D, f_\circ, m, \omega_D) \in Q_k\hat{\mathcal{A}}$ such that D_{\min} has either k or $(k - 1)$ positive edges, $\partial_C \circ p(D, f_\circ, m, \omega_D) = p \circ \partial_Q(D, f_\circ, m, \omega_D)$. The case of $(k - 1)$ positive edges will be checked in Lemma D.1, and the case of k positive edges will be checked by induction beginning the induction in Lemma D.2.

Proof of Proposition 4.6. Since ∂_C and ∂_Q are derivations and p is multiplicative with respect to the composition \circ_i , it is enough to show that $\partial_C \circ p = p \circ \partial_Q$ on fully metric diagrams in $D \in Q_*\hat{\mathcal{A}}$. We do this by induction on the number of leaves $n = \mathcal{L}(D)$. For $n = 2$, it is trivial to check that $p : Q_*\hat{\mathcal{A}} \rightarrow C_*\hat{\mathcal{A}}$ is a chain map, since in this case $\partial_Q = 0$ and $\partial_C = 0$. We now assume that $p : Q_*\hat{\mathcal{A}} \rightarrow C_*\hat{\mathcal{A}}$ is a chain map when applied to any diagram with $\mathcal{L}(D) < n$ leaves, or compositions of diagrams with $\mathcal{L}(D) < n$ leaves. We need to show the same is true for metric diagrams with $\mathcal{L}(D) = n$ leaves.

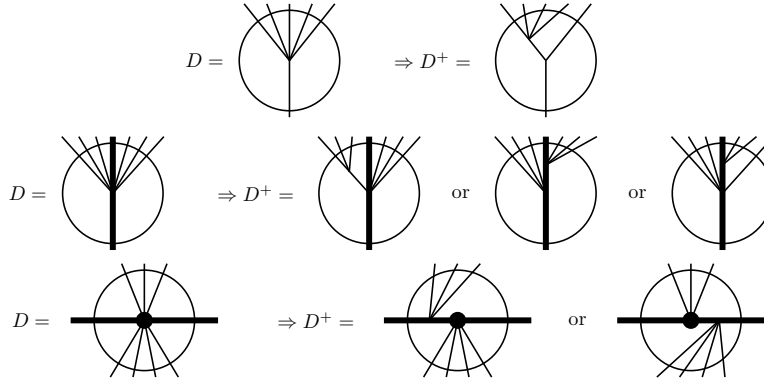
For $(D, f_\circ, m, \omega_D) \in Q_k\hat{\mathcal{A}}$ with $n = \mathcal{L}(D)$ leaves, we have by Lemma A.9(3), that $p(D, f_\circ, m, \omega_D) = 0$ when $|D_{\min}|_\oplus \neq k$. Furthermore, if $\partial_Q(D, f_\circ, m, \omega_D) = \sum_i (D_i, \dots)$ and $|(D_i)_{\min}|_\oplus \neq k - 1$ then $p(D_i, \dots) = 0$. Since ∂_Q either preserves $|\cdot|_\oplus$ or decreases it by one, we see that $|(D_i)_{\min}|_\oplus$ either equals $|D_{\min}|_\oplus$ or $|D_{\min}|_\oplus - 1$. Thus, $p(\partial_Q(D, f_\circ, m, \omega_D)) = 0$ when $|D_{\min}|_\oplus \notin \{k, k - 1\}$. In particular for $|D_{\min}|_\oplus \notin \{k, k - 1\}$, we have $p(\partial_Q(D, f_\circ, m, \omega_D)) = 0 = \partial_C(p(D, f_\circ, m, \omega_D))$. In the case of $|D_{\min}|_\oplus = k - 1$, $p(\partial_Q(D, f_\circ, m, \omega_D)) = \partial_C(p(D, f_\circ, m, \omega_D))$ is the statement of Lemma D.1 below.

It remains to check the case $|D_{\min}|_\oplus = k$. The proof is a second induction on k starting from $k = n$. If $(B, f_\circ, m, \omega_B) \in Q_n\hat{\mathcal{A}}$ is a binary diagram with $|B|_\oplus = n$, then B is the maximal binary diagram, and $p(\partial_Q(B, f_\circ, m, \omega_B)) = \partial_C(p(B, f_\circ, m, \omega_B))$ is checked in Lemma D.2 below. Thus, we may now assume $p(\partial_Q(D, f_\circ, m, \omega_D)) = \partial_C(p(D, f_\circ, m, \omega_D))$ for all $(D, f_\circ, m, \omega_D) \in Q_*\hat{\mathcal{A}}$ with either

- $\mathcal{L}(D) < n$ leaves, or compositions thereof,
- $\mathcal{L}(D) = n$ and $(D, f_\circ, m, \omega_D) \in Q_k\hat{\mathcal{A}}$ but $|D_{\min}|_\oplus \neq k$, or
- $\mathcal{L}(D) = n$ and $(D, f_\circ, m, \omega_D) \in Q_l\hat{\mathcal{A}}$ with $k < l \leq n$.

We wish to prove $p(\partial_Q(D, f_\circ, m, \omega_D)) = \partial_C(p(D, f_\circ, m, \omega_D))$ for $(D, f_\circ, m, \omega_D) \in Q_k\hat{\mathcal{A}}$ with $n = \mathcal{L}(D)$ leaves and $|D_{\min}|_\oplus = k$ (*i.e.* all k edges in D expand as positive edges).

Since D is non-binary, there exists a ternary (or higher) vertex v of D . Following [MS], we denote by D^+ the diagram given by expanding v in D in such a way that D_{\min}^+ has an extra negative edge e_v . This expansion is always possible. One approach is to use the following scheme:



Here, the diagram may be completed outside the circle in an arbitrary way, and the choice of D^+ may be determined by the number of incoming edges of a certain type.

We label the new edge e_v as metric, so that we calculate $\partial_Q(D^+, f_\circ, m, \omega) = \sum_e (D_e^+, \dots) + \sum_{e \neq e_v} (D^+/e, \dots) + (D^+/e_v, \dots)$, where D_e^+ is obtained by making the edge e non-metric, D^+/e is obtained by collapsing the edge e , and $D^+/e_v = D$. Note, that D_e^+ has a non-metric edge and is thus a composition of diagrams with fewer than n leaves, $(D^+/e, \dots) \in Q_k \hat{\mathcal{A}}$ with $|(D^+/e)_{\min}|_\oplus = k - 1$, and $(D^+, \dots) \in Q_{k+1} \hat{\mathcal{A}}$ all satisfy the chain condition $\partial_C p = p \partial_Q$ by the above hypothesis. Furthermore, (D^+, \dots) satisfying the chain condition implies the same for $\partial_Q(D^+, \dots)$, since $\partial_C p \partial_Q(D^+, \dots) = \partial_C \partial_C p(D^+, \dots) = 0 = p \partial_Q \partial_Q(D^+, \dots)$. Thus, $(D, \dots) = \partial_Q(D^+, \dots) - \sum_e (D_e^+, \dots) - \sum_{e \neq e_v} (D^+/e, \dots)$ also satisfies the chain condition. This completes the inductive step. \square

Lemma D.1. *Let $(D, f_\circ, m, \omega_D) \in Q_k \hat{\mathcal{A}}$ be a fully metric diagram (D has k metric edges) with $|D_{\min}|_\oplus = k - 1$. Then*

$$p(\partial_Q(D, f_\circ, m, \omega_D)) = 0 = \partial_C(p(D, f_\circ, m, \omega_D)).$$

Proof. Lemma A.9(3) implies that $\partial_C(p(D, f_\circ, m, \omega_D)) = 0$; it is sufficient to show that $p(\partial_Q(D, f_\circ, m, \omega_D)) = 0$. Recall that D_{\min} is given by expanding vertices in D by negative edges. Consequently, the positive edges in D_{\min} are unexpanded edges from D . Let e_1, \dots, e_{k-1} be the edges of D that become positive edges in D_{\min} , and let e_0 be the edge of D that becomes a negative edge in D_{\min} . Direct inspection shows that an edge e_0 expands to a negative edge in D_{\min} in six ways. Figure 16 shows the “local” pictures for these cases and their minima, where “local” means within a bigger diagram.

Recall from Definition 2.3 that $\partial_Q(D, f_\circ, m, \omega_D) \in Q_{k-1} \hat{\mathcal{A}}$ is given by a sum of diagrams $\sum_{i=0}^{k-1} D/e_i + \sum_{i=0}^{k-1} D_{e_i}$, where D/e_i is given by collapsing e_i , and D_{e_i} is given by relabeling e_i non-metric. Note that for $i > 0$, T_{e_i} is a composition of two diagrams along e_i . Consequently one of these two diagrams contains e_0 , giving a negative edge in its minimum, so that $p(D_{e_i}, \dots) = 0$ by Lemma A.9. Similarly, for those edges e_i such that D/e_i has less than $k - 1$ positive edges, we have $p(D/e_i, \dots) = 0$ by Lemma A.9. However, this only happens in restricted cases. First, $(D/e_0)_{\min} = D_{\min}$ so that $|(D/e_0)_{\min}|_\oplus = k - 1$, and additionally, in certain cases discussed below, it is possible that there is one more edge, denoted by e' , such that e_0 is converted to a positive edge when considering $(D/e')_{\min}$. Figure 17 illustrates this situation. To summarize, $p(D/e_i, \dots) = 0$ for all $e_i \notin \{e_0, e'\}$, and the check for $p(\partial_Q(D, f_\circ, m, \omega_D)) = 0$ reduces to two cases:

$$\begin{cases} \text{Case 1: } p(D/e_0, \dots) = p(D_{e_0}, \dots) & , \text{ when } D \text{ has no edge } e', \\ \text{Case 2: } p(D/e_0, \dots) = p(D_{e_0}, \dots) \pm p(D/e', \dots) & , \text{ when } D \text{ has an edge } e'. \end{cases}$$

Case 1: The diagrams in Figure 18 depict the situations in which this case can occur. The proof that $p(D/e_0, \dots) = p(D_{e_0}, \dots)$ now follows. Since e_0 in D_{e_0} is non-metric, D_{e_0} decomposes as

$$(D_{e_0}, f_\circ, m_{e_0}, \omega' \wedge \omega'') = \sigma \cdot ((D', f_\circ, m, \omega') \circ_{e_0} (D'', f_\circ, m, \omega'')),$$

so that

$$\begin{aligned} p(D_{e_0}, f_\circ, m_{e_0}, \omega' \wedge \omega'') &= \sigma \cdot (p(D', f_\circ, m, \omega') \circ_{e_0} p(D'', f_\circ, m, \omega'')) \\ &= \sum_{S', S''} \sigma \cdot ((S', f_\circ, \omega(S', D')) \circ_{e_0} (S'', f_\circ, \omega(S'', D''))), \end{aligned}$$

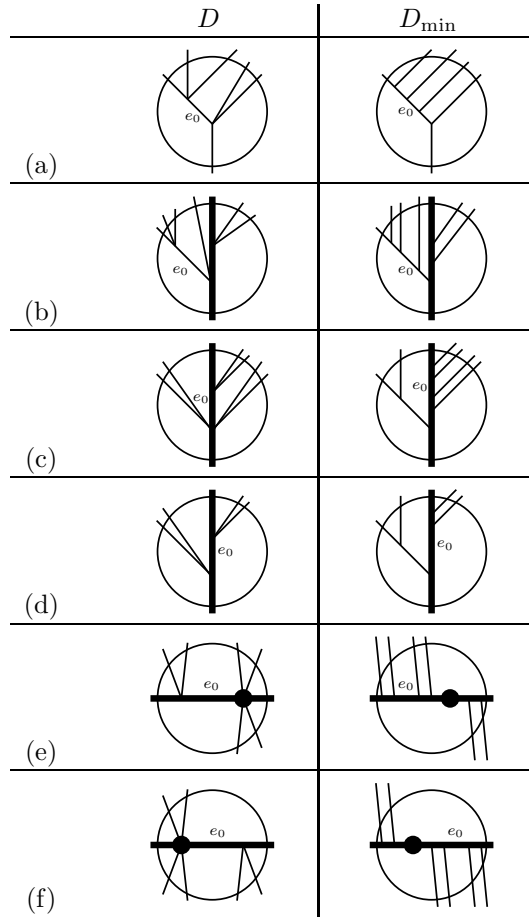


FIGURE 16. Here are the six ways for an edge to be expanded as a negative edge when considering D_{\min} .

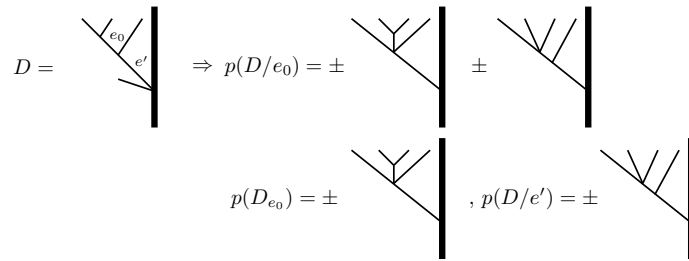


FIGURE 17. In the diagram D with edges e_0 and e' as above, we have $p(D/e_0, \dots) = \pm p(D_{e_0}, \dots) \pm p(D/e', \dots)$ and $p(D/e', \dots) = 0$.

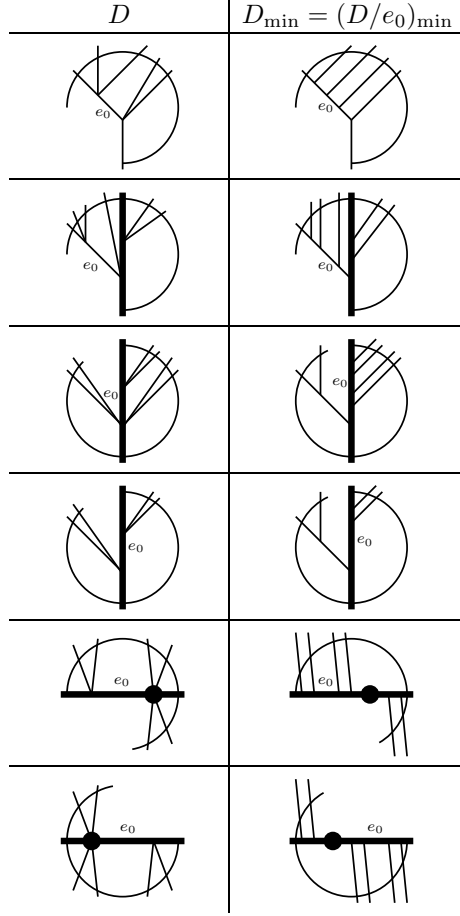
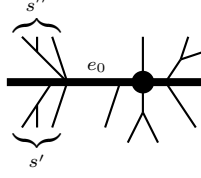


FIGURE 18. Case 1: p is non-vanishing only for D/e_0 and D_{e_0} . The open “half-circles” for D indicate that each diagram D may be completed in an arbitrary way outside the half-circle. Thus, a half-circle that connects to an edge denotes that more edges may be added on the side of the edge outside the half-circle.

where we sum over all S' and S'' with $S'_{\max} \leq D'_{\min}$ and $S''_{\max} \leq D''_{\min}$. On the other hand,

$$p(D/e_0, f_{\circlearrowleft}, m, \omega' \wedge \omega'') = \sum (S, f_{\circlearrowleft}, \omega(S, D)),$$

where we sum over all S with $S_{\max} \leq (D/e_0)_{\min} = D_{\min}$. Consequently, the equality $p(D/e_0, \dots) = p(D_{e_0}, \dots)$ follows (up to sign) by noting that each S_{\max} with $S_{\max} \leq D_{\min}$ is given by a composition along e_0 , *i.e.*, $S_{\max} = S'_{\max} \circ_{e_0} S''_{\max}$ (since, by the order relations, a change of e_0 when reducing D_{\min} also changes the number of positive edges). The proof of this case will be complete, once we compare the signs for $S' \circ_{e_0} S''$ and S . To calculate these signs, we assume that D' has r leaves and degree p with $\omega' = e'_1 \wedge \dots \wedge e'_p$, and D'' has s leaves and degree q with $\omega'' = e''_1 \wedge \dots \wedge e''_q$. Let $\xi_{D_{\min}}$, $\xi_{D'_{\min}}$ and $\xi_{D''_{\min}}$ denote the orientations from Step 1 in Appendix A.2. We first assume that $S_{\max} = D_{\min}$; then $S'_{\max} = D'_{\min}$

FIGURE 19. The composition $S' \circ_{e_0} S''$.

and $S''_{\max} = D''_{\min}$, and $\omega(S, D) = (\omega' \wedge \omega'') \rfloor \xi_{D_{\min}}$, $\omega(S', D') = \omega' \rfloor \xi_{D'_{\min}}$, and $\omega(S'', D'') = \omega'' \rfloor \xi_{D''_{\min}}$. We need to consider the cases $\sigma = id$ or $\sigma \neq id$; the latter occurs when S' is an inner product diagram and e_0 is a thick module edge on the left of S' .

- Let $\sigma = id$; then either S' is not an inner product diagram or \circ_{e_0} is not a composition at the first position. Assume e_0 composes at the i^{th} position. Then,

$$\begin{aligned} (S', f_{\circ}, \omega(S', D')) \circ_i (S'', f_{\circ}, \omega(S'', D'')) \\ = (-1)^{i(s+1)+r \cdot q} (S' \circ_{e_0} S'', f_{\circ}, (\omega' \rfloor \xi_{D'_{\min}}) \wedge (\omega'' \rfloor \xi_{D''_{\min}}) \wedge e_0). \end{aligned}$$

On the other hand, by Remark A.7, $\xi_{D_{\min}}$ is given by

$$\xi_{D_{\min}} = (-1)^{i+(i-1)(s-2)} \xi_{D'_{\min}} \wedge e_0 \wedge \xi_{D''_{\min}} = (-1)^{i(s+1)} \xi_{D'_{\min}} \wedge \xi_{D''_{\min}} \wedge e_0,$$

so that

$$\begin{aligned} \omega(S, D) &= (\omega' \wedge \omega'') \rfloor \xi_{D_{\min}} = (-1)^{i(s+1)} (\omega' \wedge \omega'') \rfloor (\xi_{D'_{\min}} \wedge \xi_{D''_{\min}} \wedge e_0) \\ &= (-1)^{i(s+1)+r \cdot q} (\omega' \rfloor \xi_{D'_{\min}}) \wedge (\omega'' \rfloor \xi_{D''_{\min}}) \wedge e_0. \end{aligned}$$

- Let $\sigma \neq id$; so that S' is an inner product diagram and the composition at e_0 is at the first position of S' . Assume that S'' is a module diagram with s' leaves to the left of the module branch, s'' leaves to the right of the module branch, and $s = s' + s'' + 1$; see Figure 19. Then as before, we obtain a sign of $(-1)^{1 \cdot (s+1)+r \cdot q}$ for the composition $S' \circ_{e_0} S''$ with orientation $(\omega' \rfloor \xi_{D'_{\min}}) \wedge (\omega'' \rfloor \xi_{D''_{\min}}) \wedge e_0$, but the cyclic permutation introduces an additional sign of $(-1)^{s'(s''+r)}$. On the other hand, Remark A.7 shows that $\xi_{D_{\min}} = (-1)^{1+(s'-2)(s''+r-2)} \xi_{D'_{\min}} \wedge e_0 \wedge \xi_{D''_{\min}}$, which can be seen by writing the $s' - 2$ edges that are attached on the lower left of e_0 in D''_{\min} at the end of $\xi_{D''_{\min}}$. Thus we obtain again the same sign as before:

$$\begin{aligned} \omega(S, D) &= (\omega' \wedge \omega'') \rfloor \xi_{D_{\min}} = (-1)^{1+s'(s''+r)} (\omega' \wedge \omega'') \rfloor (\xi_{D'_{\min}} \wedge e_0 \wedge \xi_{D''_{\min}}) \\ &= (-1)^{1+s+s'(s''+r)} (\omega' \wedge \omega'') \rfloor (\xi_{D'_{\min}} \wedge \xi_{D''_{\min}} \wedge e_0) \\ &= (-1)^{1+s+r \cdot q+s'(s''+r)} (\omega' \rfloor \xi_{D'_{\min}}) \wedge (\omega'' \rfloor \xi_{D''_{\min}}) \wedge e_0. \end{aligned}$$

For the general case $S_{\max} < D_{\min}$, note that any steps given by a local move that changes $\omega(S, D)$ correspond exactly to a local move that change $\omega(S', D')$ or $\omega(S'', D'')$ by the same sign.

Case 2: Considering those diagrams depicted in Figure 16 such that e_0 is the only negative edge, Figure 20 shows the situations in which Case 2 occurs. (Here, the cases that are symmetric with respect to a 180° symmetry, such as cases (e)

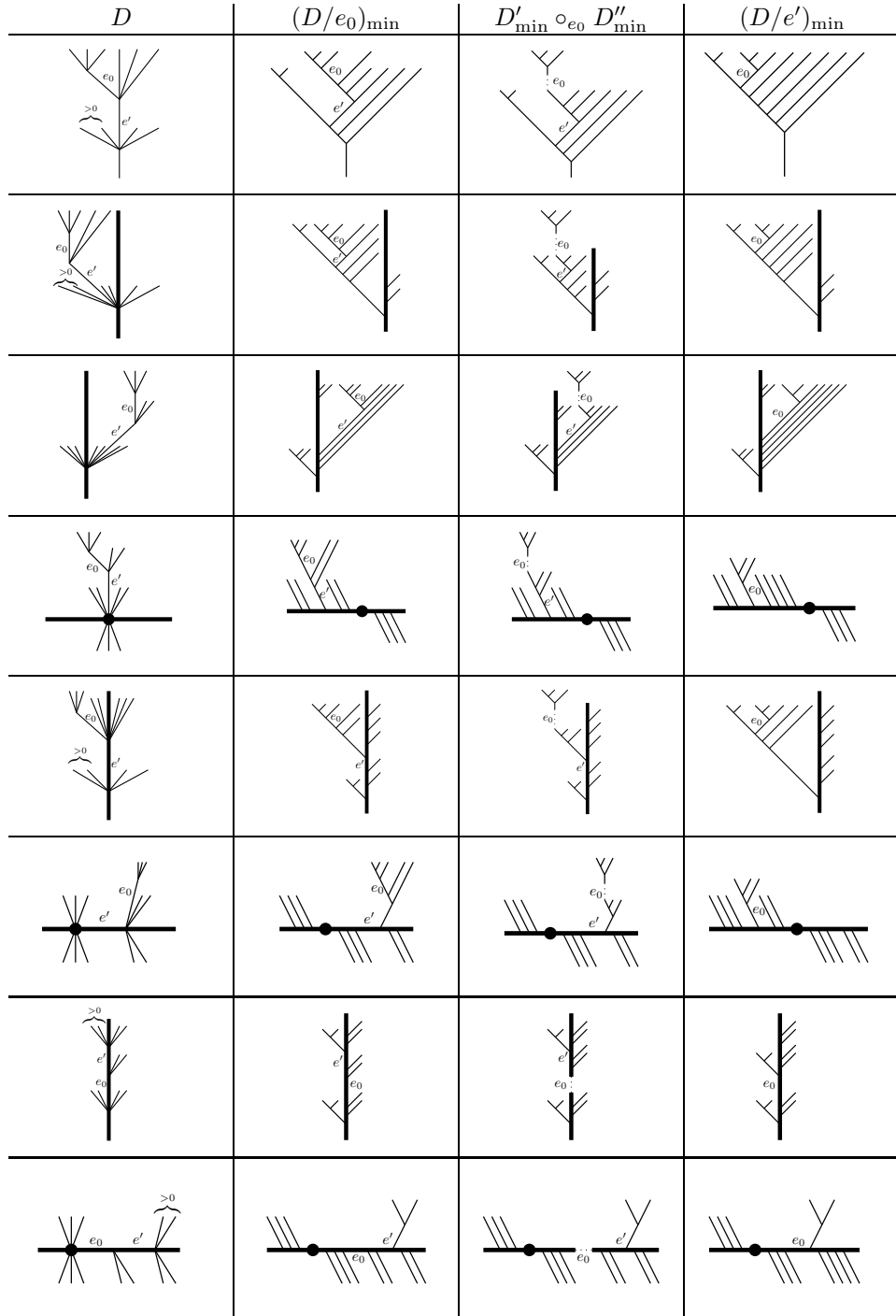


FIGURE 20. Case 2: p is non-vanishing for D/e_0 , D_{e_0} , and D/e' . Each of these diagrams may be completed in an arbitrary way. (To improve readability, the circle that were drawn in the previous diagrams have been omitted here.)

and (f) in Figure 16, have been excluded.) As in Case 1 above, $p(D/e_0, \dots) = \sum_{S_{\max} \leq D_{\min}} (S, \dots)$. This sum contains all the terms that appear in

$$\begin{aligned} p(D/e_0, \dots) &= p(D' \circ_{e_0} D'', \dots) = \sigma \cdot p(D', \dots) \circ_{e_0} p(D'', \dots) \\ &= \sum_{S'_{\max} \leq D'_{\min}, S''_{\max} \leq D''_{\min}} (S', \dots) \circ_{e_0} (S'', \dots), \end{aligned}$$

where the signs can be checked as in Case 1. However, $p(D/e_0, \dots)$ can now have more terms. In fact, a direct inspection shows that the binary diagrams $S_{\max} \leq (D/e_0)_{\min}$ from Figure 20 are of two types: (1) those with terms using no local moves from Definition A.3 for e_0 , and (2) those with terms that use local moves. The first type is given by $p(D/e_0, \dots)$; the second type is given by $p(D/e', \dots)$.

It only remains to check that the induced signs for $p(D/e_0, \dots)$ and $p(D/e', \dots)$ cancel. We first assume that $S_{\max} = (D/e')_{\min}$. Denote the orientation for D by $\omega_D = \omega_R \wedge e_0 \wedge e'$, where ω_R stands for the orientation of the remaining edges in D . With this, the two terms D/e_0 and D/e' appear with opposite signs,

$$\partial_Q(D, f_{\cup}, m, \omega_D) = \pm \left((D/e_0, f_{\cup}, m, \omega_{D/e_0}) - (D/e', f_{\cup}, m, \omega_{D/e'}) \right) + \dots,$$

where $\omega_{D/e_0} = \omega_R \wedge e'$ and $\omega_{D/e'} = \omega_R \wedge e_0$. We claim that $p(D/e_0, f_{\cup}, m, \omega_{D/e_0}) = p(D/e', f_{\cup}, m, \omega_{D/e'})$. By assumption $S_{\max} = (D/e')_{\min}$; let us calculate the induced orientations $\omega(S, D/e_0)$ and $\omega(S, D/e')$ and show they coincide.

Note, that in each of the cases from Figure 20, there is a unique path of local moves from $(D/e_0)_{\min} = D_{\min}$ to $(D/e')_{\min}$ that preserves the number of positive edges. This path is determined by a sequence of edges e_1, \dots, e_j to which we apply the local moves. For example, in the first row in Figure 20, this sequence is depicted as e_1, e_2 on the left of Figure 21. Now, write $\xi_{D_{\min}}$ in the form $\xi_{D_{\min}} = e' \wedge e_1 \wedge \dots \wedge e_j \wedge e_0 \wedge \xi_R$

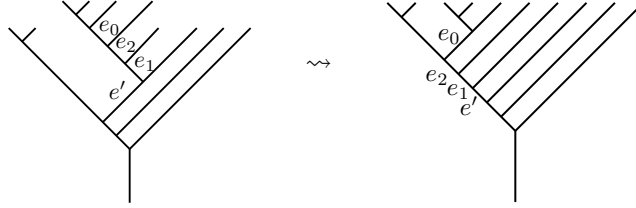


FIGURE 21. Local moves change $(D/e_0)_{\min}$ to $(D/e')_{\min}$.

where ξ_R is the orientation on the remaining edges. In order to calculate $\omega(S, D/e_0)$ we need to perform a sequence of moves on e', e_1, \dots, e_j as depicted in Figure 21. At the i^{th} local move, the i^{th} orientation ξ_i changes by a factor of -1 , so that $\xi_i = (-1)^i \cdot e' \wedge e_1 \wedge \dots \wedge e_j \wedge e_0 \wedge \xi_R$. Keeping track of the positive edge, while making local moves, tells us that e_i is positive after the i^{th} move. After $j+1$ steps, we obtain the orientation $\xi_{j+1} = (-1)^{j+1} \cdot e' \wedge e_1 \wedge \dots \wedge e_j \wedge e_0 \wedge \xi_R$ which applies to the diagram $S_{\max} = (D/e')_{\min}$, as depicted on the right of Figure 21 with positive edge e_0 so that the orientation induced from ω_{D/e_0} is now $\omega_R \wedge e_0$. With this, we calculate $\omega(S, D/e_0) = (\omega_R \wedge e_0) \lrcorner \xi_{j+1} = \omega_R \lrcorner (e' \wedge e_1 \wedge \dots \wedge e_j \wedge \xi_R)$.

On the other hand, we see from Remark A.7, that $\xi_{(D/e')_{\min}} = (-1)^{j+1} \cdot e' \wedge e_1 \wedge \cdots \wedge e_j \wedge e_0 \wedge \xi_R$. Since $\omega_{D/e'} = \omega_R \wedge e_0$, we obtain $\omega(S, D/e') = (\omega_R \wedge e_0) \lrcorner \xi_{(D/e')_{\min}} = \omega_R \lrcorner (e' \wedge e_1 \wedge \cdots \wedge e_j \wedge \xi_R)$, which coincides with $\omega(S, D/e_0)$.

The cases where $S_{\max} < (D/e')_{\min}$ apply the same local moves and change the signs in $p(D/e_0, \dots)$ and $p(D/e', \dots)$ the same way, establishing equality of $\omega(S, D/e_0) = \omega(S, D/e')$.

This completes the sign check for Case 2, and with this the proof of the lemma. \square

Lemma D.2. *Let $(B, f_\cup, m, \omega_B^{\text{std}}) \in Q_n \hat{A}$ be a maximal binary diagram, i.e. one of the following three diagrams,*

$$(T_n)_{\max} = \begin{array}{c} \diagup \quad \diagdown \\ \diagup \quad \diagdown \\ \diagup \quad \diagdown \\ \diagup \quad \diagdown \\ | \end{array}, \quad (M_{k,l})_{\max} = \begin{array}{c} \diagup \quad \diagdown \\ \diagup \quad \diagdown \\ \diagup \quad \diagdown \\ \diagup \quad \diagdown \\ \text{---} \\ | \end{array}, \quad (I_{k,l})_{\max} = \begin{array}{c} \diagup \quad \diagdown \\ \diagup \quad \diagdown \\ \diagup \quad \diagdown \\ \text{---} \\ \text{---} \\ | \end{array}.$$

Then, $\partial_C \circ p(B, f_\cup, m, \omega_B^{\text{std}}) = p \circ \partial_Q(B, f_\cup, m, \omega_B^{\text{std}})$.

Proof. We show $\partial_C \circ p = p \circ \partial_Q$ when applied to $B = (T_n)_{\max}$, $B = (M_{k,l})_{\max}$, and $B = (I_{k,l})_{\max}$ by direct computation. Note that for any corolla c , Lemma 4.5(ii) gives

$$\partial_C(p(c_{\max}, f_\cup, m, \omega_B^{\text{std}})) = \partial_C(c, f_\cup, +1) = \sum_{D/e=c} (D, f_\cup, +e).$$

We need to evaluate $p(\partial_Q(c_{\max}, f_\cup, m, \omega_B^{\text{std}}))$. To simplify notation, we will often ignore the label f_\cup and express the quadruple as a diagram together with its orientation.

The first case $B = (T_n)_{\max}$ appears in [MS] (see [MS, Figures 6 and 7]),

$$\begin{array}{ccc} \begin{array}{c} \diagup \quad \diagdown \\ \diagup \quad \diagdown \\ \diagup \quad \diagdown \\ \diagup \quad \diagdown \\ | \\ e_1 \end{array} & \xrightarrow{p} & \begin{array}{c} \diagup \quad \diagdown \\ \diagup \quad \diagdown \\ \diagup \quad \diagdown \\ \diagup \quad \diagdown \\ | \end{array} \\ \partial_Q \downarrow & & \downarrow \partial_C \\ \partial_Q((T_n)_{\max}) & \xrightarrow{p} & \sum_{r \geq 2} \sum_{s \geq 0} T_n^{r,s}, \end{array}$$

where $\omega_{(T_n)_{\max}}^{\text{std}} = e_1 \wedge \cdots \wedge e_{n-2}$ and

$$\begin{array}{l} T_n^{r,s} = \begin{array}{c} \overbrace{\diagup \quad \diagdown}^r \\ \overbrace{\diagup \quad \diagdown}^s \\ \diagup \quad \diagdown \\ \diagup \quad \diagdown \\ | \end{array} \text{ with orientation } e; \text{ and} \\ \partial_Q((T_n)_{\max}) = \sum_{\text{edge } e_j} (-1)^j \left(\begin{array}{c} \diagup \quad \diagdown \\ \diagup \quad \diagdown \\ \diagup \quad \diagdown \\ \diagup \quad \diagdown \\ | \end{array} \omega_j - \begin{array}{c} \diagup \quad \diagdown \\ \diagup \quad \diagdown \\ \diagup \quad \diagdown \\ \diagup \quad \diagdown \\ | \end{array} \omega_j \right), \end{array}$$

where the edge e_j is collapsed, so that $\omega_j = e_1 \wedge \cdots \wedge \widehat{e}_j \wedge \cdots \wedge e_{n-2}$. Here, the thick edge labeled “ n ” denotes a non-metric edge. Note that

$$p \left(\sum_j (-1)^j \left(\begin{array}{c} \text{Diagram of } \omega_j \end{array} \right) \omega_j \right) = \sum_r \sum_{s>0} T_n^{r,s}.$$

The sign calculation for B/e_j is the same for all three cases $B = (T_n)_{\max}, (M_{k,l})_{\max}$ and $(I_{k,l})_{\max}$. Since we make one edge move from B to $(B/e_j)_{\min}$, we have:

$$\begin{aligned} \xi_{(B/e_j)_{\min}} &= (-1)^1 \cdot (-1)^{1+2+\cdots+(n-3)} e_1 \wedge \cdots \wedge e_j \wedge \cdots \wedge e_{n-2} \\ &= (-1)^{(1+\cdots+(n-3))+(n-2)-j+1} e_1 \wedge \cdots \wedge \widehat{e}_j \wedge \cdots \wedge e_{n-2} \wedge e_j \\ &= (-1)^{(1+\cdots+(n-2))-j} e_1 \wedge \cdots \wedge \widehat{e}_j \wedge \cdots \wedge e_{n-2} \wedge e_j. \end{aligned}$$

$$\text{Thus } \omega(T_n^{r,s}, B/e_j) = (-1)^j \omega_j \lrcorner \xi_{(B/e_j)_{\min}} = +e_j.$$

On the other hand,

$$p \left(\sum_j (-1)^{j+1} \left(\begin{array}{c} \text{Diagram of } \omega_j \text{ with thick edge } n \end{array} \right) \omega_j \right) = \sum_r T_n^{r,0},$$

with the sign calculated as follows: Denote by B' and B'' the subtrees of B_{e_j} such that $B_{e_j} = B' \circ_{e_j} B''$. Then $\omega_{B'}^{\text{std}} = e_1 \wedge \cdots \wedge e_{j-1}$ and $\omega_{B''}^{\text{std}} = e_{j+1} \wedge \cdots \wedge e_{n-2}$ so that

$$(B_{e_j}, f_{\circlearrowleft}, m_{e_j}, \omega_j) = (B', f_{\circlearrowleft}, m, \omega_{B'}^{\text{std}}) \circ_{j+1} (B'', f_{\circlearrowleft}, m, \omega_{B''}^{\text{std}})$$

$$\begin{aligned} \text{Thus } (-1)^{j+1} p(B_{e_j}, f_{\circlearrowleft}, m_{e_j}, \omega_j) &= (-1)^{j+1} p(B', f_{\circlearrowleft}, m, \omega_{B'}^{\text{std}}) \circ_{j+1} p(B'', f_{\circlearrowleft}, m, \omega_{B''}^{\text{std}}) \\ &= (-1)^{j+1} (c', f_{\circlearrowleft}, +1) \circ_{j+1} (c'', f_{\circlearrowleft}, +1) \\ &= (-1)^{j+1+(j+1)(n-j+1)+(j+1)(n-2-j)} (c' \circ_{e_j} c'', f_{\circlearrowleft}, +e_j) \\ &= (c' \circ_{e_j} c'', f_{\circlearrowleft}, +e_j). \end{aligned}$$

Next, we consider the case $B = (M_{k,l})_{\max}$. We will show that the following diagram commutes:

$$\begin{array}{ccc} \begin{array}{c} \text{Diagram of } (M_{k,l})_{\max} \text{ with edges } e_1, \dots, e_{k+l-1} \end{array} & \xrightarrow{p} & \begin{array}{c} \text{Diagram of } \partial_C \end{array} \\ \downarrow \partial_Q & & \downarrow \partial_C \\ \partial_Q((M_{k,l})_{\max}) & \xrightarrow{p} & \sum_{r,s} M_{k,l}^{r,s} + \sum_{r,s} N_{k,l}^{r,s} + \sum_{r,s} O_{k,l}^{r,s} \end{array}$$

where $\omega_{(M_{k,l})_{\max}}^{\text{std}} = (-1)^k \cdot e_1 \wedge \cdots \wedge e_{k+l-1}$; and the module trees

$$M_{k,l}^{r,s} = \begin{array}{c} \text{Diagram of } M_{k,l}^{r,s} \text{ with } r \text{ and } s \text{ subtrees} \end{array}$$

$$\begin{aligned}
\text{Thus } p(B_{e_1}, f_{\circlearrowleft}, m_{e_1}, \omega_1) &= (-1)^{kl+l+1} p(B', f_{\circlearrowleft}, m, \omega_{B'}^{\text{std}}) \circ_1 p(B'', f_{\circlearrowleft}, m, \omega_{B''}^{\text{std}}) \\
&= (-1)^{kl+l+1} (c', f_{\circlearrowleft}, +1) \circ_1 (c'', f_{\circlearrowleft}, +1) \\
&= (-1)^{kl+l+1+1+(k+1+1)+(l+1)(k-1)} (c' \circ_{e_1} c'', f_{\circlearrowleft}, +e_1) \\
&= (c' \circ_{e_1} c'', f_{\circlearrowleft}, +e_1).
\end{aligned}$$

Furthermore,

$$p \left(\sum_j (-1)^j \begin{array}{c} \text{diagram} \\ \text{diagram} \end{array} \right) = \sum_{r>0} \sum_s O_{k,l}^{r,s} + \sum_r \sum_{0<s<l} M_{k,l}^{r,s}$$

and

$$p \left(\sum_j (-1)^{j+1} \begin{array}{c} \text{diagram} \\ \text{diagram} \end{array} \right) = \sum_s O_{k,l}^{0,s}.$$

Write $B_{e_j} = B' \circ_{e_j} B''$. Then $\omega_{B'}^{\text{std}} = (-1)^k \cdot e_1 \wedge \cdots \wedge e_{j-1}$, and $\omega_{B''}^{\text{std}} = e_{j+1} \wedge \cdots \wedge e_{k+l-1}$, so that

$$(B_{e_j}, f_{\circlearrowleft}, m_{e_j}, \omega_j) = (B', f_{\circlearrowleft}, m, \omega_{B'}^{\text{std}}) \circ_{j+1} (B'', f_{\circlearrowleft}, m, \omega_{B''}^{\text{std}}).$$

$$\begin{aligned}
\text{Thus } (-1)^{j+1} p(B_{e_j}, f_{\circlearrowleft}, m_{e_j}, \omega_j) &= (-1)^{j+1} p(B', f_{\circlearrowleft}, m, \omega_{B'}^{\text{std}}) \circ_{j+1} p(B'', f_{\circlearrowleft}, m, \omega_{B''}^{\text{std}}) \\
&= (-1)^{j+1} (c', f_{\circlearrowleft}, +1) \circ_{j+1} (c'', f_{\circlearrowleft}, +1) \\
&= (-1)^{j+1+(j+1)(k+l+1-j+1)+(j+1)(k+l-1-j)} (c' \circ_{e_j} c'', f_{\circlearrowleft}, +e_j) \\
&= (c' \circ_{e_j} c'', f_{\circlearrowleft}, +e_j).
\end{aligned}$$

Finally, we consider $B = (I_{k,l})_{\max}$. We will show the following diagram commutes:

$$\begin{array}{ccc}
\begin{array}{c} \text{diagram} \\ \text{diagram} \end{array} & \xrightarrow{p} & \begin{array}{c} \text{diagram} \\ \text{diagram} \end{array} \\
\downarrow \partial_Q & & \downarrow \partial_C \\
\partial_Q((I_{k,l})_{\max}) & \xrightarrow{p} & \sum_{r,s} I_{k,l}^{r,s} + \sum_{r,s} J_{k,l}^{r,s} + \sum_{r,s} K_{k,l}^{r,s} + \sum_{r,s} L_{k,l}^{r,s},
\end{array}$$

where $\omega_{(I_{k,l})_{\max}}^{\text{std}} = (-1)^l \cdot e_1 \wedge \cdots \wedge e_{k+l}$, and

$$\begin{array}{cc}
I_{k,l}^{r,s} = \begin{array}{c} \text{diagram} \\ \text{diagram} \end{array} & J_{k,l}^{r,s} = \begin{array}{c} \text{diagram} \\ \text{diagram} \end{array} \\
K_{k,l}^{r,s} = \begin{array}{c} \text{diagram} \\ \text{diagram} \end{array} & L_{k,l}^{r,s} = \begin{array}{c} \text{diagram} \\ \text{diagram} \end{array}
\end{array}$$

have orientation $+e$, with e being the unique edge in the diagram. Now, $\partial_Q((I_{k,l})_{\max})$ equals

$$\begin{aligned} &= (-1) \begin{array}{c} | \\ \bullet \\ \hline \text{////} \end{array} - (-1) \begin{array}{c} | \\ \bullet \\ \hline \text{////} \\ n \end{array} + \sum_{e_j} (-1)^j \left(\begin{array}{c} | \\ \bullet \\ \hline \text{////} \\ \text{////} \end{array} - \begin{array}{c} | \\ \bullet \\ \hline \text{////} \\ n \end{array} \right) \\ &+ (-1)^{k+1} \begin{array}{c} | \\ \bullet \\ \hline \text{////} \\ \text{////} \end{array} - (-1)^{k+1} \begin{array}{c} | \\ \bullet \\ \hline \text{////} \\ n \end{array} + \sum_{e_j} (-1)^j \left(\begin{array}{c} | \\ \bullet \\ \hline \text{////} \\ \text{////} \end{array} - \begin{array}{c} | \\ \bullet \\ \hline \text{////} \\ n \end{array} \right). \end{aligned}$$

Again, all of these terms have orientation $\omega_j = (-1)^l \cdot e_1 \wedge \cdots \wedge \widehat{e_j} \wedge \cdots \wedge e_{k+l-1}$. We evaluate p as follows. First,

$$p \left((-1) \begin{array}{c} | \\ \bullet \\ \hline \text{////} \end{array} \right) = \sum_s I_{k,l}^{1,s}$$

and

$$p \left(\begin{array}{c} | \\ \bullet \\ \hline \text{////} \\ n \end{array} \right) = J_{k,l}^{k,0}.$$

Writing $B_{e_1} = B' \circ_{e_1} B''$ gives $\omega_{B'}^{\text{std}} = (-1)^l \cdot e_{k+1} \wedge \cdots \wedge e_{k+l}$ and $\omega_{B''}^{\text{std}} = e_2 \wedge \cdots \wedge e_k$. This gives

$$\begin{aligned} (B_{e_1}, f_\circ, m_{e_1}, \omega_1) &= (-1)^{l(k-1)} (B', f_\circ, m, \omega_{B'}^{\text{std}}) \circ_2 (B'', f_\circ, m, \omega_{B''}^{\text{std}}). \\ \text{Thus } p(B_{e_1}, f_\circ, m_{e_1}, \omega_1) &= (-1)^{l(k-1)} p(B', f_\circ, m, \omega_{B'}^{\text{std}}) \circ_2 p(B'', f_\circ, m, \omega_{B''}^{\text{std}}) \\ &= (-1)^{l(k-1)} (c', f_\circ, +1) \circ_2 (c'', f_\circ, +1) \\ &= (-1)^{l(k-1)+2(k+1)+l(k+1)} (c' \circ_{e_1} c'', f_\circ, +e_1) \\ &= (c' \circ_{e_1} c'', f_\circ, +e_1). \end{aligned}$$

Second,

$$p \left(\sum_j (-1)^j \begin{array}{c} | \\ \bullet \\ \hline \text{////} \end{array} \right) = \sum_{r \geq 2} \sum_s I_{k,l}^{r,s} + \sum_r \sum_s K_{k,l}^{r,s}$$

and

$$p \left(\sum_j (-1)^{j+1} \begin{array}{c} | \\ \bullet \\ \hline \text{////} \\ n \end{array} \right) = \sum_{r < k} J_{k,l}^{r,0}.$$

Writing $B_{e_j} = B' \circ_{e_j} B''$ gives $\omega_{B'}^{\text{std}} = (-1)^l \cdot e_1 \wedge \cdots \wedge e_{j-1} \wedge e_{k+1} \wedge \cdots \wedge e_{k+l}$, and $\omega_{B''}^{\text{std}} = e_{j+1} \wedge \cdots \wedge e_k$. This gives,

$$\begin{aligned} (B_{e_j}, f_\circ, m_{e_j}, \omega_j) &= (-1)^{l(k-j)} (B', f_\circ, m, \omega_{B'}^{\text{std}}) \circ_{j+1} (B'', f_\circ, m, \omega_{B''}^{\text{std}}) \\ \text{Thus } (-1)^{j+1} p(B_{e_j}, f_\circ, m_{e_j}, \omega_j) &= (-1)^{j+1+l(k+j)} p(B', f_\circ, m, \omega_{B'}^{\text{std}}) \circ_{j+1} p(B'', f_\circ, m, \omega_{B''}^{\text{std}}) \\ &= (-1)^{j+1+l(k+j)} (c', f_\circ, +1) \circ_{j+1} (c'', f_\circ, +1) \\ &= (-1)^{j+1+l(k+j)+(j+1)(k-j+2+1)+(l+j+1)(k-j)} \\ &\quad (c' \circ_{e_j} c'', f_\circ, +e_j) \end{aligned}$$

$$= (c' \circ_{e_j} c'', f_{\circlearrowleft}, +e_j).$$

Third,

$$p \left((-1)^{k+1} \begin{array}{c} \text{////} \quad \bullet \quad \text{////} \\ \text{---} \\ \text{////} \end{array} \right) = \sum_r J_{k,l}^{r,1}$$

and

$$p \left((-1)^k \begin{array}{c} \text{////} \quad n \quad \bullet \quad \text{////} \\ \text{---} \\ \text{////} \end{array} \right) = I_{k,l}^{0,l}.$$

Writing $B_{e_{k+1}} = \sigma \cdot (B' \circ_{e_{k+1}} B'')$ gives $\omega_{B'}^{\text{std}} = e_1 \wedge \cdots \wedge e_k$, and $\omega_{B''}^{\text{std}} = e_{k+2} \wedge \cdots \wedge e_{k+l}$, where $\sigma \in S_{k+l+2}$ is the cyclic permutation “ $+(l+1) \pmod{k+l+2}$ ”. This gives,

$$(B_{e_{k+1}}, f_{\circlearrowleft}, m_{e_{k+1}}, \omega_j) = (-1)^l \cdot \sigma \cdot ((B', f_{\circlearrowleft}, m, \omega_{B'}^{\text{std}}) \circ_1 (B'', f_{\circlearrowleft}, m, \omega_{B''}^{\text{std}})).$$

$$\begin{aligned} \text{Thus } (-1)^k p(B_{e_{k+1}}, f_{\circlearrowleft}, m_{e_{k+1}}, \omega_j) &= (-1)^{k+l} \sigma \cdot (p(B', f_{\circlearrowleft}, m, \omega_{B'}^{\text{std}}) \circ_1 p(B'', f_{\circlearrowleft}, m, \omega_{B''}^{\text{std}})) \\ &= (-1)^{k+l} \sigma \cdot ((c', f_{\circlearrowleft}, +1) \circ_1 (c'', f_{\circlearrowleft}, +1)) \\ &= (-1)^{k+l+1(l+1+1)+(k+2)(l-1)} \\ &\quad \sigma \cdot (c' \circ_{e_{k+1}} c'', f_{\circlearrowleft} \circ \sigma^{-1}, +e_{k+1}) \\ &= (c' \circ_{e_{k+1}} c'', f_{\circlearrowleft}, +e_{k+1}). \end{aligned}$$

Fourth,

$$p \left(\sum_j (-1)^j \begin{array}{c} \text{////} \quad \bullet \quad \text{////} \\ \text{---} \\ \text{////} \end{array} \right) = \sum_r \sum_{s \geq 2} J_{k,l}^{r,s} + \sum_r \sum_s L_{k,l}^{r,s}$$

and

$$p \left(\sum_j (-1)^{j+1} \begin{array}{c} \text{////} \quad n \quad \bullet \quad \text{////} \\ \text{---} \\ \text{////} \end{array} \right) = \sum_{s < l} I_{k,l}^{0,s}.$$

Writing $B_{e_j} = \sigma \cdot (B' \circ_{e_j} B'')$ gives $\omega_{B'}^{\text{std}} = (-1)^{j-k-1} \cdot e_1 \wedge \cdots \wedge e_{j-1}$, and $\omega_{B''}^{\text{std}} = e_{j+1} \wedge \cdots \wedge e_{k+l}$, where $\sigma \in S_{k+l+2}$ is the cyclic permutation “ $+(k+l+1-j) \pmod{k+l+2}$ ”. This gives,

$$(B_{e_j}, f_{\circlearrowleft}, m_{e_j}, \omega_j) = (-1)^{l+j-k-1} \sigma \cdot ((B', f_{\circlearrowleft}, m, \omega_{B'}^{\text{std}}) \circ_1 (B'', f_{\circlearrowleft}, m, \omega_{B''}^{\text{std}})).$$

$$\begin{aligned} \text{Thus } (-1)^{j+1} p(B_{e_j}, f_{\circlearrowleft}, m_{e_j}, \omega_j) &= (-1)^{k+l} \sigma \cdot (p(B', f_{\circlearrowleft}, m, \omega_{B'}^{\text{std}}) \circ_1 p(B'', f_{\circlearrowleft}, m, \omega_{B''}^{\text{std}})) \\ &= (-1)^{k+l} \sigma \cdot ((c', f_{\circlearrowleft}, +1) \circ_1 (c'', f_{\circlearrowleft}, +1)) \\ &= (-1)^{k+l+1 \cdot (k+l-j+2+1) + (j+1)(k+l-j)} \\ &\quad \sigma \cdot (c' \circ_{e_j} c'', f_{\circlearrowleft} \cdot \sigma^{-1}, +e_j) \\ &= (-1)^{(j+1)(k+l-j+1)} \sigma \cdot (c' \circ_{e_j} c'', f_{\circlearrowleft} \cdot \sigma^{-1}, +e_j) \\ &= (c' \circ_{e_j} c'', f_{\circlearrowleft}, +e_j). \end{aligned}$$

This completes the proof the lemma. \square

REFERENCES

- [BV] J.M. Boardman, R.M. Vogt, *Homotopy invariant algebraic structures on topological spaces*, Springer LNM 347, 1973
- [C] C.-H. Cho, *Strong homotopy inner product of an A-infinity algebra*, Int. Math. Res. Not., no. 41, 2008
- [L] J.-L. Loday, *The diagonal of the Stasheff polytope*, preprint arXiv:0710.0572v2
- [LT] R. Longoni, T. Tradler, *Homotopy Inner Products for Cyclic Operads*, Journal of Homotopy and Related Structures, vol. 3(1), 2008, pp. 343-358, 2008
- [MacL] S. Mac Lane, *Categories for the Working Mathematician*, Springer, Graduate Texts in Mathematics 5, 1971
- [MS] M. Markl, S. Shnider, *Associahedra, cellular W-construction and products of A_∞ algebras*, Trans. of the AMS, Vol. 358, No. 6, pp. 2353-2372, 2005
- [SU] S. Saneblidze, R. Umble, *Diagonals on the Permutohedra, Multiplihedra and Associahedra*, Homology, Homotopy and Applications, vol.6(1), pp.363-411, 2004
- [S] J. Stasheff, *Homotopy Associativity of H-Spaces. I*, Trans. AMS, Vol. 108, No. 2, pp. 275-292, 1963
- [Ta] D. Tamari, *The algebra of bracketings and their enumeration*, Nieuw Arch. Wisk. (3) 10, 1962, pp. 131-146.
- [TT] J. Terilla, T. Tradler, *Deformations of associative algebras with inner products*, Homology, Homotopy, and Applications 8(2), p. 115-131, 2006
- [T1] T. Tradler, *Infinity Inner Products on A-Infinity Algebras*, Journal of Homotopy and Related Structures, vol. 3(1), pp. 245-271, 2008
- [T2] T. Tradler, *The BV Algebra on Hochschild Cohomology Induced by Infinity Inner Products*, Annales de L'institut Fourier, vol. 58, no. 7, p. 2351-2379, 2008
- [TZ] T. Tradler, M. Zeinalian, *Algebraic String Operations*, K-Theory, vol. 38, no. 1, 2007

THOMAS TRADLER, DEPARTMENT OF MATHEMATICS, COLLEGE OF TECHNOLOGY, CITY UNIVERSITY OF NEW YORK, 300 JAY STREET, BROOKLYN, NY 11201, USA, AND MAX-PLANCK-INSTITUT FÜR MATHEMATIK, VIVATSGASSE 7, 53111 BONN, GERMANY

E-mail address: ttradler@citytech.cuny.edu

DEPARTMENT OF MATHEMATICS, MILLERSVILLE UNIVERSITY OF PENNSYLVANIA, MILLERSVILLE, PA. 17551

E-mail address: ron.umble@millersville.edu